arXiv:2206.11654v1 [cs.DS] 23 Jun 2022

Hierarchical Agglomerative Graph Clustering in Poly-Logarithmic Depth

Laxman Dhulipala
Google Research and
University of Maryland
laxman@umd.edu

David Eisenstat
Google Research
eisen@google.com

Jakub Łącki
Google Research
jlacki@google.com

Vahab Mirrokni
Google Research
mirrokni@google.com

Jessica Shi
MIT CSAIL
jeshi@mit.edu

Abstract

Obtaining scalable algorithms for *hierarchical agglomerative clustering* (HAC) is of significant interest due to the massive size of real-world datasets. At the same time, efficiently parallelizing HAC is difficult due to the seemingly sequential nature of the algorithm. In this paper, we address this issue and present ParHAC, the first efficient parallel HAC algorithm with sublinear depth for the widely-used average-linkage function. In particular, we provide a $(1+\epsilon)$-approximation algorithm for this problem on m edge graphs using $\tilde{O}(m)$ work and poly-logarithmic depth. Moreover, we show that obtaining similar bounds for *exact* average-linkage HAC is not possible under standard complexity-theoretic assumptions.

We complement our theoretical results with a comprehensive study of the ParHAC algorithm in terms of its scalability, performance, and quality, and compare with several state-of-the-art sequential and parallel baselines. On a broad set of large publicly-available real-world datasets, we find that ParHAC obtains a 50.1x speedup on average over the best sequential baseline, while achieving quality similar to the exact HAC algorithm. We also show that ParHAC can cluster one of the largest publicly available graph datasets with 124 billion edges in a little over three hours using a commodity multicore machine.

1 Introduction

Hierarchical Agglomerative Clustering (HAC) [48, 50, 70] is a fundamental and widely-used clustering method with numerous applications in unsupervised learning, community detection, and biology. Given n input points, the HAC algorithm starts by forming a separate cluster for each input point, and proceeds in $n-1$ steps. Each step replaces the two most *similar* clusters by its union. The exact notion of similarity between two clusters is specified by a configurable *linkage function*. This function is typically given all pairwise similarities between points from the two clusters. Some of the most popular choices are *average-linkage* (the arithmetic mean of all similarities), *single-linkage* (the maximum similarity), and *complete-linkage* (the minimum similarity). Among these, average-linkage is of particular importance, as it is known to find high-quality clusters in real-world applications [25, 54, 55, 64]. [1]

[1] We note that HAC can also be defined in terms of input points and *dissimilarities* between the points. We discuss and compare both settings in Section 1.2

Preprint. Under review.

Although HAC has been of significant interest to statisticians, computer scientists, and clustering practitioners since the 1960s, applying HAC to very large datasets remains a major challenge. A significant source of difficulty is the need to compute all pairwise similarities between sets of points, which HAC implementations typically perform at the start of the algorithm at the expense of $\Theta(n^2)$ work and space [57, 58, 72]. To address this difficulty, two directions have recently been explored in the literature. The first has focused on designing approximate sub-quadratic work algorithms in the dissimilarity setting, using sketching and approximate nearest neighbor (ANN) techniques [4, 56]. The second approach focuses on the *similarity-graph setting*, and is what we build on in this paper. Here, the idea is to build a (typically sparse) similarity graph over the pointset input, e.g., by representing each point as a vertex, connecting a point to its k most similar neighbors, and then applying a graph-based HAC algorithm on this similarity graph [37].[2] Surprisingly, despite only using a sub-quadratic number of similarities, similarity graph-based HAC algorithms can match or sometimes even surpass the quality of an algorithm using the full $O(n^2)$ similarity matrix [37].

Prior works on these approaches [4, 37] give provable guarantees on the quality of the resulting approximation algorithms; in fact, both yield $(1+\epsilon)$-approximate HAC algorithms, as proposed by [56]. Specifically, a $(1+\epsilon)$-*approximate HAC algorithm* is an algorithm in which each step only merges edges that have similarity at least $\mathcal{W}_{\max}/(1+\epsilon)$ where $\mathcal{W}_{\max}$ is currently the largest similarity.[3] Hence, an $(1+\epsilon)$-approximate algorithm is constrained to merge an edge that is "close" in similarity to the merge that the exact algorithm would perform. At the same time, the algorithm has flexibility in which edge to merge, which can potentially be algorithmically exploited.

Despite the progress on scaling up HAC, further improvements appeared challenging due to the seemingly inherently sequential nature of the HAC algorithm [8, 54]. Several recent attempts at parallelizing HAC either rely on optimistic assumptions on the input [71, 75], significantly diverge from the original algorithm, potentially impacting quality [8, 23, 54], or deliver weak approximation guarantees [56]. Understanding if HAC can be solved in sub-quadratic work and poly-logarithmic depth (or even polynomial work and sub-linear depth) has thus remained an intriguing open question, even when allowing for approximation.

1.1 Our Contributions

In this paper, we introduce the first efficient parallel algorithm computing $(1+\epsilon)$-approximate average-linkage HAC with poly-logarithmic depth and near-linear total work. We use the standard *work-depth model* of parallel computation [14, 26] to analyze the theoretical cost of our algorithm, where briefly, the *work* is the total number of operations performed, and the *depth* is the longest chain of dependencies. The algorithm takes as input a similarity graph, which contains n vertices (representing input points) and m weighted edges (representing nonzero similarities between points).

Theorem 1.1. *There is a parallel $(1+\epsilon)$-approximate average-linkage graph-based HAC algorithm that given a similarity graph containing n vertices and m weighted edges runs in $\tilde{O}(m+n)$ work in expectation and has $O(\log^4 n)$ depth with high probability.*[4]

For a fixed ϵ, our algorithm, which we call ParHAC, runs in poly-logarithmic depth and $\tilde{O}(m)$-work. Thus, it is work-efficient up to logarithmic factors and achieves high parallelism (ratio of work to depth). We note that the same setting, i.e., parametrizing the input size by the number of *nonzero* similarities, has been recently studied in the sequential case [37], where an $\tilde{O}(m)$-work sequential $(1+\epsilon)$-approximate algorithm is known. Prior to our result, no average-linkage HAC algorithm with sublinear depth was known (even allowing approximation).

On the negative side, we show that allowing approximation is necessary, as obtaining an average-linkage *exact* HAC algorithm with poly-logarithmic depth is not possible under standard complexity-theory assumptions (i.e., it is a P-complete problem). In other words, an exact polynomial-work parallel HAC algorithm for average-linkage in poly-logarithmic depth would imply poly-logarithmic depth algorithms for *all* problems solvable in polynomial time (i.e., show that $\mathsf{P} = \mathsf{NC}$). Our lower

[2] We note that [37] introduce both an exact algorithm for average-linkage HAC running in $O(n\sqrt{m})$ work and an approximate algorithm running in $\tilde{O}(m)$ work. We define $\tilde{O}(f(x)) := O(f(x)\mathsf{polylog}(f(x)))$.

[3] We note that [56] deals with dissimilarities, but we adapt the definition to similarities in the natural way.

[4] An algorithm has $O(f(n))$ cost with high probability (*whp*) if it has $O(k \cdot f(n))$ cost with probability at least $1 - 1/n^k$.

bound formalizes a commonly held belief that the algorithm is inherently sequential [71] and justifies studying the approximate variant of HAC.

Theorem 1.2. *Graph-based HAC using average-linkage is* P*-complete.*

We complement our theoretical results by providing an efficient parallel implementation of ParHAC, and comparing it with existing graph-based and pointset-based HAC baselines across a broad set of publicly available real-world datasets. For scalability, we show that ParHAC achieves strong speedups relative to other high-quality HAC baselines, achieving 50.1x average speedup over the approximate sequential algorithm from [37] when run on a 72-core machine. Moreover, we study the overall running times of using ParHAC in the pointset setting, and find that ParHAC can cluster significantly larger datasets compared to fastcluster [58], a state-of-the-art pointset clustering algorithm, and achieves up to 417x speedup over fastcluster in end-to-end running time.

We show that the above speedups are achieved without loss (or even with gain) for the final algorithm. In particular, for the Adjusted Rand-Index quality measure, we find that the quality of ParHAC is on average 3.1% better than the best approximate sequential baseline, and is on average within 3.69% of the best score for any method on the datasets that we study. Finally, we find that ParHAC achieves consistently strong quality results on three other quality metrics that we study compared with the best solutions offered by exact and approximate algorithms.

We plan to make our implementations publicly available on GitHub.

1.2 Graph-Based Hierarchical Agglomerative Clustering

As mentioned earlier in the introduction, our focus in this paper is on clustering (typically sparse) weighted graphs where the edge weights represent similarities between vertices. More formally, we study parallel algorithms for the *graph-based hierarchical agglomerative clustering (HAC)* problem, which takes as input a graph $G = (V, E, w)$ and proceeds by repeatedly merging the two most similar clusters, where the similarity is given by a configurable linkage function. Equivalently, this process can be viewed in terms of a graph H, whose vertices are clusters, and edges represent clusters of positive similarity (in particular, the edge weights give the similarities between clusters). Initially, when all clusters have size 1, H is equal to G. Each operation of merging two clusters corresponds to contracting an edge of H (we call this operation a *merge*). In the following we typically use this alternative view of the algorithm.

The output of the algorithm is a *dendrogram* – a rooted binary tree that has a single leaf for each vertex in the input graph, with internal nodes corresponding clusters obtained by merges, and the weights of internal nodes representing the similarity of the corresponding merge that formed it.

We focus on the *average-linkage measure*, which assumes that the similarity between two clusters (X, Y) is equal to $\sum_{(x,y)\in \mathsf{Cut}(X,Y)} w(x, y)/(|X| \cdot |Y|)$, that is, the total weight of edges between X and Y, divided by the maximum number of possible edges between the clusters. Throughout this paper, we consider graphs with arbitrary positive edge weights representing similarities. We discuss other linkage measures in the Appendix.

A natural question is, why use similarities instead of dissimilarities? Both settings have been previously considered in the literature, and although it hard to argue that one approach is "better" than the other, our primary reason for studying similarities is because the similarity setting is arguably a more natural setting for clustering *sparse* graphs. Specifically, it is natural to assume that the similarity between pairs of vertices not connected by an edge is 0, whereas no such assignment of a dissimilarity to missing edges is obvious when edge weights represent dissimilarities.

1.3 Related Works

ParHAC is inspired by a recent sequential $(1+\epsilon)$-approximate average-linkage HAC algorithm, which runs in $\tilde{O}(m)$ time [37]. However, obtaining a theoretically-efficient and practical parallel algorithm requires significant new ideas. The evaluation of [37] studied the difference in quality between exact and $(1 + \epsilon)$-approximate HAC and showed that even moderately small $\epsilon = 0.1$ maintains the quality of exact HAC. Our results on the quality of ParHAC are consistent with these findings.

Efficient parallelizations of HAC are known in the case of single-linkage (essentially equivalent to maximum spanning forest), and centroid linkage, if one allows $O(\log^2 n)$-approximation [56].

In other cases, the existing parallelizations of exact HAC either use linear depth [59], much larger work [28, 61] or do not come with any bounds on the running time [45, 71, 75]. The ParChain framework [75] for parallel exact HAC on pointsets recently showed that average-linkage HAC can be solved in hours for million-point datasets. Very recently, it was shown that a *distributed* implementation of the RAC algorithm can exactly cluster a billion-point dataset in a few hours using 200 machines and 3200 CPUs [71]. However, the depth of the algorithm is linear in the worst case, and can be large in practice.

In order to scale hierarchical clustering to large datasets, several HAC-inspired algorithm have been proposed, including Affinity clustering [8] and SCC [54]. Both algorithms are designed for a distributed setting, in which the number of computation rounds that one can afford is highly constrained. In particular, SCC can be seen as a best-effort approximation of HAC, given a fixed (usually small) number of rounds to run. We implemented both algorithms (using the framework that we built to develop ParHAC) and included them in our empirical evaluation.

The theoretical foundations of HAC has been developed in recent years [22, 27, 55], and have motivated using HAC in real-world settings [20, 21, 24, 25, 63]. The version of HAC that takes a graph as input has also been studied before, especially in the context of graphs derived from point sets [40, 41, 47], although without strong theoretical guarantees. Another line of work by Abboud et al. [4] showed that if the input points are in the Euclidean space and the Ward linkage method is used [74], approximate HAC can be solved in subquadratic time.

2 Parallel Approximate HAC

In this section we describe our parallel HAC algorithm, which we call ParHAC. We assume that the input is a weighted graph $G = (V, E, w)$, where $w : E \to \mathbb{R}^+$ gives the edge weights.

Let us now provide some background for the main ideas behind ParHAC. As observed in [71, 75], a simple exact parallel HAC algorithm can be obtained almost directly from the 40-year-old nearest-neighbor chain algorithm [9]. The parallel algorithm finds all edges xy such that xy is the highest-weight incident edge to each endpoint, x and y. For simplicity, we assume here that all edge weights are distinct. One can see that these edges form a matching (which does not necessarily match all vertices), and the correctness of the nearest-neighbor chain algorithm implies that if the endpoints of these edges are merged in parallel, the output is equivalent to what a sequential HAC algorithm produces. Following [71], we call this algorithm reciprocal agglomerative clustering (RAC). Clearly, the amount of parallelism in RAC is data-dependent. In particular, it can take a linear number of steps in the worst case [71], and, as we find in our experiments, up to 21,081 steps on the YouTube (YT) real-world graph with just 1.1M vertices and 5.9M edges.

Once we consider $(1+\epsilon)$-approximate HAC, the set of edges that we can choose to merge in the first step *grows* to include all edges whose weight is within $(1+\epsilon)$ factor of $\mathcal{W}_{\max}$, the largest edge weight in the graph. Let us call these edges $(1+\epsilon)$-*heavy*. A major challenge is that the $(1+\epsilon)$-heavy edges no longer form a matching, and thus cannot be all merged in parallel. To see this, consider an example where all $(1+\epsilon)$-heavy edges have a common endpoint x. Once one vertex merges with x, the size of the cluster represented by x increases, which decreases the weights of all edges incident to x, and as a result some of these edges may cease to be $(1+\epsilon)$-heavy.

Considering the $(1+\epsilon)$-heavy edges motivates the use of ***geometric layering***, a technique where we group the edges into layers based on their weights and process edges in the same layer in parallel (e.g., see [10, 12]). In more detail, let $\mathcal{W}_{\max}$ and $\mathcal{W}_{\min}$ be the maximum-weight and minimum-weight in the graph, respectively. The i-th layer contains all edges with weight between $((1+\epsilon)^{-(i+1)} \cdot \mathcal{W}_{\max}, (1+\epsilon)^{-i} \cdot \mathcal{W}_{\max}]$. ParHAC processes the layers one at a time; to compute the next layer it computes the maximum weight edge in the graph $W_{\max}$, and processes all edges between $((1+\epsilon)^{-1} W_{\max}, W_{\max}]$. We refer to an iteration of this loop as a ***layer-contraction phase***.

Let us now describe how to implement a layer-contraction phase. The pseudocode for the procedure is shown in Algorithm 1. The goal is to merge $(1+\epsilon)$-heavy edges in parallel until none are left. The main challenge is in ensuring that the algorithm does not violate the approximation requirements. An ***outer-round*** of Algorithm 1 begins by randomly coloring active (i.e., non-isolated) vertices either red or blue (Line 3), assigning each color with probability $1/2$. Then, it constructs a graph G_c which consists of edges of G of weight belonging to the current layer (Line 5). Moreover, G_c only contains

Algorithm 1 ParHAC-ContractLayer($G = (V, E, w), T_L, \epsilon, D$)

Input: Similarity graph, G, threshold T_L, $\epsilon > 0$, dendrogram D.
Ensure: All edges in G have weight $< T_L$.

1: Let $W_{\max}$ be the current maximum-weight edge in G.
2: **while** $W_{\max} \geq T_L$ **do** ▷ Outer round
3: Randomly color active vertices of G either red or blue.
4: Let R, B be the sets of red and blue vertices respectively.
5: Let $G_c = (V, E_c, w)$, where E_c contains all edges in G that have weight $\geq T_L$, and connect a vertex $x \in B$ with a vertex $y \in R$, where the size of y is not smaller than the size of x.
6: **while** $|E_c| > 0$ **do** ▷ Inner round
7: Select a random priority π_b for $b \in B$.
8: Let C_b be a random red neighbor for each $b \in B$.
9: Let $T = \{(C_b, \pi_b, b) \mid b \in B\}$. Sort T lexicographically.
10: Let T_r be triples from T with first component equal to r.
11: For each $r \in R$, select the first prefix of T_r, in which the total size of blue vertices exceeds $\epsilon|r|$
12: Let M be the set of (red, blue) vertex pairs selected.
13: Merge vertices in G and G_c based on the pairs from M, updating edge weights in G_c.
14: Remove edges of G_c that have two red endpoints or weight below T_L
15: Update D based on M. If multiple $b \in B$ merge to a single $r \in R$, merge them into r in the sorted order.
16: Remove $r \in R$ from G_c whose cluster size grew by more than a $(1 + \epsilon)$ factor since the start of the outer round.
17: Recompute $W_{\max}$ based on the current state of G.

edges whose endpoints have different colors, and whose red endpoint has larger size than the blue endpoint. Observe that each edge of G is added to G_c with probability at least $1/4$. The algorithm then performs inner-rounds while the number of edges in G_c is non-zero.

Let us now describe a single ***inner-round*** (Lines 6–16). The goal of an inner round is for many blue vertices to merge into red vertices. Here we allow multiple blue vertices to merge with a single red vertex. A key property (also exploited in [37]) is that as long as the size of the cluster represented by x does not grow too much within a single round, the weights of the edges incident to x are very close to what they were in the beginning of the round. Specifically, assume that (in the beginning of a round) x represents a cluster of size c. Then, until the size of this cluster exceeds $(1 + \epsilon) \cdot c$, the edges incident to x that were $(1 + \epsilon)$-heavy at the beginning of the round remain (at least) $(1 + \epsilon)^2$-heavy. This allows us to merge multiple vertices with x in a single round, at the cost of increasing the approximation ratio to $(1 + \epsilon)^2$ (which can be reduced to $(1 + \epsilon)$ by scaling ϵ by a constant factor).

More specifically, an inner round is implemented as follows. For each blue vertex $b \in B$, the algorithm selects a uniformly random priority $\pi_b \in [0, 1]$ (Line 7) which is used to perform symmetry breaking when merging vertices. It then chooses a random red neighbor, C_b, for each $b \in B$ (Line 8). If a blue vertex has no red neighbors it will not participate in the subsequent steps, but for simplicity when describing the algorithm we assume that each $b \in B$ has a valid C_b. The algorithm then builds T, a set of triples for each $b \in B$ containing the value of its candidate red neighbor C_b, its priority π_b, and its id, b (Line 9), and sorts this set lexicographically. We call the elements of T *proposals*. At this point, a red vertex may have proposals to merge from a large number of blue neighbors, and so the algorithm selects for each $r \in R$ the first prefix of T_r (the merges proposing to r) whose total cluster size exceeds $\epsilon|r|$ (Lines 10–11). If no prefix of T_r has this property, the algorithm selects all of T_r.

Finally, the algorithm gathers all of the (r, b) vertex pairs that were selected (Line 12) and applies these merges to update both G and G_c (Line 13). Note that after this update we remove all edges of G_c that have two red endpoints, and as a result we maintain the invariant that each edge of G_c has two endpoints of distinct colors, and the size of the red endpoint is at least the size of the blue one.

2.1 Theoretical Analysis

We show that our algorithm performs nearly-linear total work, has poly-logarithmic depth, and thus polynomial parallelism, and has good approximation guarantees. For the purpose of this analysis we assume that $\epsilon > 0$ is a constant. We provide proofs in the Appendix and outline the main ideas here.

We start by analyzing a layer-contraction phase, and bound the total work and number of rounds required. We start by showing that within each inner round of Algorithm 1, each blue vertex makes progress in expectation either by being merged, or by having many edges incident to it be deleted.

Lemma 2.1. *Consider an arbitrary blue vertex b within an inner round. Within this round either (a) a constant factor of edges incident to b are deleted, or (b) with constant probability b is merged into one of its red neighbors.*

Using this property, we can bound the number of inner rounds within an outer round to be $O(\log n)$ *whp*. Next, we show that the number of outer rounds is also $O(\log n)$ *whp*.

Lemma 2.2. *The number of outer rounds in a call to Algorithm 1 is $O(\log n)$ with high probability.*

The proof works by showing that for each edge e of the graph G_c at the beginning of the loop, either (a) the endpoints of e are merged together, or (b) the weight of e drops below T_L, or (c) an endpoint of e increases its size by a factor of $(1 + \epsilon)$.

Finally, assuming the aspect-ratio $\mathcal{A} = \mathcal{W}_{\max}/\mathcal{W}_{\min} = O(\mathsf{poly}(n))$, the number of layer-contraction phases is $O(\mathsf{polylog}(n))$.[5] Putting all of the previous results together and implementing the algorithm using standard parallel primitives in the work-depth model, we obtain the following result:

Theorem 2.3. ParHAC *is a $(1 + \epsilon)$-approximate algorithm for average-linkage HAC that runs in $\tilde{O}(m + n)$ work in expectation and has $O(\log^4(n))$ depth with high probability.*

2.2 Lower Bound

We complement our upper bound with a parallel hardness result for *exact* graph-based average-linkage HAC. Since the problem is in P, we show P-hardness to show the P-completeness result. Specifically, we give an NC reduction from the P-complete monotone circuit-value problem (monotone CVP) by transforming a monotone circuit into a graph-based HAC instance such that two vertices are merged into the same cluster with a given merge similarity if and only if a target output gate evaluates to true. With minor modifications, our reduction extends to the show the P-completeness of a variant of average-linkage called WPGMA-linkage; we provide our constructions and proofs in the Appendix.

2.3 Algorithm Implementation

We implemented ParHAC in C++ using the *CPAM* (Compressed Parallel Augmented Maps) framework [38], which provides compressed and highly space-efficient ordered maps and sets. We build on CPAM's implementation of the Aspen framework [33, 38], which provides a compressed dynamic graph representation that supports efficient parallel updates (batch edge insertions and deletions).

Compressed Clustered Graph Representation. In practice ParHAC can perform a large number of rounds per-layer in the case where ϵ is small (e.g., $\epsilon = 0.01$). Although updating the entire graph on each of these rounds is theoretically-efficient (the algorithm will only perform $\tilde{O}(m + n)$ work), many of these rounds only merge a small number of vertices, and leave the majority of the edges unaffected, and so updating the entire graph each round can be highly wasteful.

Instead, we designed an efficient *compressed clustered graph representation* using the CPAM framework [38] which enables us to update the underlying similarity graph in work proportional to the number of merged vertices and their incident neighbors, rather than proportional to the total number of edges in the graph. Importantly, using CPAM enables lossless compression for integer-keyed maps to store the cluster adjacency information using just a few bytes per edge.[6] We provide more details about the representation and the supported operations in the Appendix.

[5] All existing HAC approximation algorithms make similar assumptions on the aspect ratio [4, 37].

[6] We obtain a 2.9x space savings using our CPAM-based implementation over an optimized hashtable-based implementation of a clustered graph; the running times of both implementations are essentially the same.

Other Hierarchical Graph Clustering Algorithms. Our new clustered graph representation makes it very easy to implement other parallel graph clustering algorithms. In particular, we developed a faithful version of the Affinity clustering algorithm [8] and the recently proposed SCC algorithm [54] (which is essentially a thresholded version of Affinity) using a few dozens of lines of additional code. Both algorithms are essentially heuristics that are designed to mimic the behavior of HAC, while running in very few rounds (an important constraint for the distributed environments these algorithms are designed for). We note that most of the work done by these algorithms is the work required to merge clusters in the underlying graph, and so by using the same primitives for merging graphs, we eliminate a significant source of differences when comparing algorithms.

3 Empirical Evaluation

Experimental Setup. We ran all of our experiments on a 72-core Dell PowerEdge R930 (with two-way hyper-threading) with 4×2.4GHz Intel 18-core E7-8867 v4 Xeon processors (with a 4800MHz bus and 45MB L3 cache) and 1TB of main memory. Our programs use a lightweight work-stealing parallel scheduler [5, 13]. Further details about our setup and input data can be found in the Appendix.

HAC Algorithms Evaluated. We compare ParHAC with several HAC baselines. SeqHAC is the approximate sequential average-linkage algorithm that was recently introduced [37]. ParHAC$_{\mathcal{E}}$ and SeqHAC$_{\mathcal{E}}$ are exact versions of the ParHAC and SeqHAC algorithms, where the ParHAC code takes $T_L = W_{\max}$ in each layer-contraction phase and sets $\epsilon = 0$ (i.e., the layer only consists of equal-weight edges). ParHAC$_{0.1}$ and SeqHAC$_{0.1}$ both use $\epsilon = 0.1$. We also evaluate our implementation of Affinity clustering [8] and the recently developed SCC algorithm [54], which we refer to as ParAffinity and ParSCC$_{sim}$. Both these algorithms can be thought of as heuristic parallelizations of the HAC algorithm, which are designed with speed and good parallelization properties in mind. We describe these in more detail in the Appendix. Lastly, we also compare the graph-based implementations of HAC to pointset-based HAC implementations from the scipy package using the single-, complete-, average-, and Ward-linkage measures. These are exact HAC algorithms, which look at the complete similarity matrix and thus require time which is at least quadratic in the input size.

Building Similarity Graphs from Pointsets. Some of our experiments generate graphs from a pointset by computing the approximate nearest neighbors (ANN) of each point, and converting the distances to similarities. We convert distances to similarities using the formula $\mathsf{sim}(u, v) = \frac{1}{1+\mathsf{dist}(u,v)}$. We then reweight the similarities by dividing each similarity by the maximum similarity. We compute the k-approximate nearest neighbors using a shared-memory parallel implementation of the *Vamana* approximate nearest neighbors (ANN) algorithm [44] with parameters $R = 75, L = 100, Q = \max(L, k)$. We discuss more details about the process in the Appendix.

3.1 Quality Evaluation

We start by investigating the quality of ParHAC with respect to ground-truth clusterings. Our goal is to understand (1) whether ParHAC preserves the clustering quality of exact average-linkage HAC (using a complete similarity matrix), and (2) what value of ϵ to use in practice. The results in this sub-section affirmatively answer (1), and show that a value of $\epsilon = 0.1$ achieves comparable quality to exact average-linkage HAC, which prior works have identified as a state-of-the-art hierarchical clustering method and use as their primary quality baseline [8, 37, 54].

We evaluate our algorithms on the *iris*, *wine*, *digits*, and *cancer*, and *faces* classification datasets from the UCI dataset repository (found in the sklearn.datasets package). We run all of the graph-based clustering algorithms on similarity graphs generated from the input pointsets using $k = 10$ in the approximate k-NN construction. We run the scipy pointset clustering algorithms directly on the input pointsets. To measure quality, we use the *Adjusted Rand-Index (ARI)* and *Normalized Mutual Information (NMI)* scores, as well as the *Dendrogram Purity* measure of a hierarchical clustering [42] which we define in the Appendix. We also study the unsupervised *Dasgupta Cost* [27] measure. We give definitions of the measures in the Appendix.

Results. We present a table of our results in the Appendix and summarize our findings here. Our main finding is that ParHAC$_{0.1}$ achieves consistently high-quality results across all of the quality

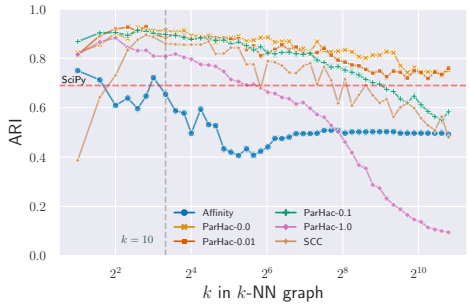


Figure 1: ARI score on the *digits* point dataset as a function of the k used in graph building. ParHAC using $\epsilon = 0.1$ is the green line using $+$ markers. The gray vertical line highlights the values for $k = 10$, which is the value of k we use in our detailed quality evaluation in the Appendix. The red horizontal line is the ARI of SciPy's average-linkage.

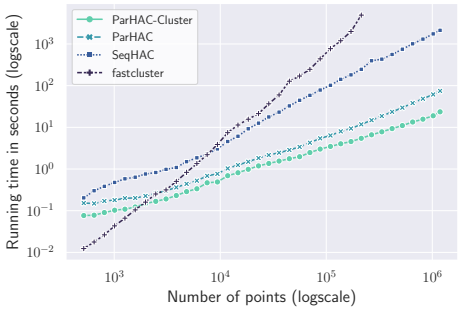


Figure 2: End-to-end running times of fastcluster's unweighted average-linkage, SeqHAC using $\epsilon = 0.1$, and ParHAC using $\epsilon = 0.1$ and 144 hyper-threads on varying-size slices of the glove-100 dataset. The time for SeqHAC and ParHAC includes the cost of solving ANN and generating the input similarity graph; ParHAC-Cluster shows only the clustering time. We terminated methods that run for more than 3 hours.

measures. For instance, for the ARI measure, $\text{ParHAC}_{0.1}$ is on average within 1.5% of the best ARI score for each graph (and achieves the best score for one of the graphs). For the NMI measure, $\text{ParHAC}_{0.1}$ is on average within 1.3% of the best NMI score for each graph (and again achieves the best score for two of the graphs). $\text{ParHAC}_{0.1}$ also achieves good results for the dendrogram purity and Dasgupta cost measures. For purity, it is on average within 1.9% of the best purity score for each graph, achieving the best score for one of the graphs, and for the unsupervised Dasgupta cost measure it is on average within 1.03% of the smallest Dasgupta cost score for each graph.

Compared with the SciPy average-linkage which is an exact HAC algorithm running on the underlying pointset, $\text{ParHAC}_{0.1}$ achieves 14.4% better ARI score on average, 3.6% better NMI score on average, 4.7% better dendrogram purity on average, and 1.02% larger Dasgupta cost on average. Compared to the best quality result obtained by either SCC_{sim} or Affinity, $\text{ParHAC}_{0.1}$ consistently obtains better quality results, achieving 35.6% better ARI score on average, 12.1% better NMI score on average, 6.7% better dendrogram purity on average, and 3.1% better Dasgupta cost on average.

Overall, we find that ParHAC achieves consistently high quality results across the four quality measures that we evaluate. Our results show that being more faithful to the HAC algorithm allows ParHAC to obtain meaningful quality gains over Affinity and SCC_{sim}.

Results with Varying k. When converting a pointset input to the similarity setting using the k-NN approach as in this paper, what value of k is required to achieve high quality? We studied each of the quality measures for the studied algorithms as a function of the k used in the k-NN construction, and present our full results for each measure and each dataset in the Appendix. Here, Figure 1 shows a representative result for the ARI measure on the digits point dataset.

We find that even modest values of k yield very high quality results and can *significantly outperform exact metric HAC algorithms* on the original pointset. Furthermore, even tripling, or increasing k an order of magnitude either yields negligible improvement for most quality measures, or in fact degrades the quality. For example, for ParHAC with $\epsilon = 0.1$, using $k = 100$ is 10% worse than using $k = 10$, and using $k = 1000$ is 47% worse than $k = 10$. Our results suggest a twofold benefit from using a graph-based approach: (1) since small values of k are sufficient for high quality results, the inputs to the clustering algorithm can be smaller, resulting in faster running times, and (2) the overall clustering quality is higher with small inputs and can lead to significant improvements over using more similarities (or using the full dissimilarity matrix, as in pointset clustering algorithms).

3.2 Evaluation on Large Real-World Graphs

Next, we evaluated ParHAC's scalability on large real-world graphs, including both social network graphs, as well as sparse, high-diameter networks. We note that the Hyperlink (HL) graph is one of the largest publicly-available graphs and contains 1.7B vertices and 125B edges. Additional details and experiments can be found in the supplementary material; we summarize them:

(1) ParHAC achieves betewen 25.7–61.3x speedup over its running time on a single thread.

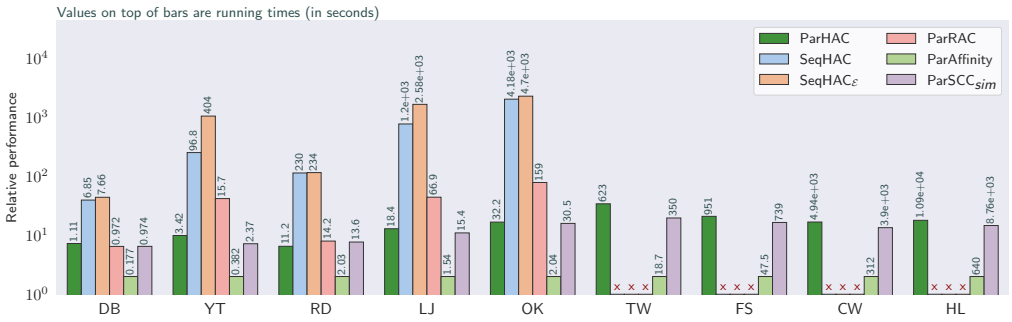


Figure 3: Relative performance of our ParHAC algorithm compared to other graph-HAC and HAC-inspired algorithms. We prefix new implementations developed in this paper with the Par prefix. The values on top of each bar show the running time of each algorithm in seconds. The times shown for the parallel algorithms are 144 hyper-thread times. We run the ParHAC and SeqHAC algorithm using $\epsilon = 0.1$. We terminated algorithms that ran longer than 6 hours and mark them with a red x.

(2) We evaluated the running time of ParHAC when the edge weights in the graph are selected based on structural properties of the input, e.g., the degree, or the number of triangles closed by the edge. Overall, we evaluated 6 highly-different weighting schemes, and find that the gap between the fastest and slowest schemes per-graph is at most 5x.
(3) Running ParHAC with larger values of ϵ consistently results in lower running times, due to the fewer number of rounds used for large ϵ.

Figure 3 shows the relative performance and of ParHAC compared with the SeqHAC and SeqHAC$_\mathcal{E}$ algorithms, and our implementations of the RAC, Affinity, and SCC$_{\text{sim}}$ algorithms. We see that our Affinity implementation is always the fastest on our graph inputs. This is due to the low theoretical and empirical round-complexity of Affinity. Compared with Affinity, SCC$_{\text{sim}}$, which runs Affinity with weight thresholding using 100 iterations is an average of 11.5x slower than Affinity due to the cost of the additional iterations. Compared to Affinity and SCC$_{\text{sim}}$, ParHAC is an average of 14.8x slower than our Affinity implementation and 1.24x slower than our SCC$_{\text{sim}}$ implementation. The speed difference between ParHAC and Affinity is due to the larger number of fine-grained rounds required by ParHAC. However, as we showed in Section 3.1, the faster running time of affinity clustering and SCC$_{\text{sim}}$ comes at the cost of significantly lower quality.

Compared with methods that implement exact or $1 + \epsilon$-approximate HAC, ParHAC is significantly faster. Compared with SeqHAC and SeqHAC$_\mathcal{E}$, ParHAC obtains 50.1x and 86.4x speedup on average respectively. Compared with RAC, ParHAC achieves an average speedup of 7.1x on the graphs that RAC can successfully complete within the time limit. Although RAC is faster than ParHAC on two of our small graph inputs, it requires a very large number of rounds on the remaining graphs.

To the best of our knowledge, our results are the first to show that graphs with tens to hundreds of billions of edges can be clustered in a matter of tens of minutes (using heuristics like Affinity and SCC$_{\text{sim}}$ with fewer iterations) to hours (using SCC$_{\text{sim}}$ with many iterations, or methods with approximation guarantees such as ParHAC). Recently, results on trillion-edge similarity graphs have been reported [54, 71]. Due to the memory requirements of storing such large datasets in memory, ParHAC may not be directly applicable; however, it may be possible to design a distributed $(1 + \epsilon)$-approximate HAC algorithm with low round-complexity by building on the ideas in this paper.

Discussion. To the best of our knowledge, our results are the first to show that graphs with tens to hundreds of billions of edges can be clustered in a matter of tens of minutes (using heuristic methods like Affinity and SCC$_{\text{sim}}$ with fewer iterations) to hours (using SCC$_{\text{sim}}$ with many iterations or methods with approximation guarantees such as ParHAC). We are not aware of other shared-memory clustering results that work at this large scale. Our theoretically-efficient implementations can be viewed as part of a recent line of work showing that theoretically-efficient shared-memory parallel graph algorithms can scale to the largest publicly available graphs using a modest amount of resources [31–33, 35, 65, 66].

3.3 Pointset Clustering: End-to-End Evaluation

We conclude by evaluating the performance of ParHAC in the case when the input is a pointset. In this setting, in order to use a graph-based HAC algorithm, one needs to construct a similarity graph before running the clustering algorithm. As a baseline, we use the average-linkage HAC implementation from fastcluster [58], which takes a pointset input. We compare with fastcluster as we found it yields more consistent (and slightly faster) performance for larger numbers of points than the implementations in sklearn and SciPy.[7] We also compare ParHAC to the SeqHAC algorithm in this setting, where SeqHAC uses the same similarity-graph building method as ParHAC described earlier in this section, and both algorithms are run using $\epsilon = 0.1$.

We run our end-to-end experiment on the Glove-100 dataset, which is a 100-dimensional dataset containing vector-embeddings for 1.18 million words. Figure 2 shows the results of our experiment. We stress that the running times of the graph-based algorithms (SeqHAC and ParHAC) include the time spent building the graph. First, we found that for $n > 3000$, the end-to-end times of ParHAC are always faster than the time taken by fastcluster, and for $n > 9400$, the end-to-end times of SeqHAC are always faster than the time taken by fastcluster. Comparing fastcluster on the largest slice of the Glove-100 dataset it can solve in under three hours with the graph-based methods, SeqHAC is 20x faster, and ParHAC is 417x faster.

4 Conclusion

In this paper we have introduced ParHAC, the first parallel algorithm for hierarchical agglomerative graph clustering using the average-linkage measure that has strong theoretical-bounds on its work and depth, as well as provable approximation guarantees. We have shown that ParHAC scales to massive real-world graphs with tens to hundreds of billions of edges on a single machine and achieves high-quality results compared to existing graph-based and pointset-based hierarchical clustering methods.

An interesting question for future work is whether we can reduce the round complexity of our algorithm to make it more suitable for distributed settings. Another interesting question is to compare the running time and quality of bottom-up HAC methods for size-constrained clustering and balanced partitioning problems, which typically rely on top-down methods [7**?** , 19, 30, 46]. Although it has recently been shown that it may not be possible to design algorithms for incremental and dynamic HAC with good worst-case guarantees [73], it would be interesting to design practical $(1 + \epsilon)$-approximations for these settings, potentially building on ideas from ParHAC.

References

[1] Chem dataset. `https://archive.ics.uci.edu/ml/datasets/Gas+sensor+array+under+dynamic+gas+mixtures`.

[2] Geolife dataset. `https://www.microsoft.com/en-us/research/publication/geolife-gps-trajectory-dataset-user-guide/`.

[3] Uci1 dataset. `https://archive.ics.uci.edu/ml/datasets/magic+gamma+telescopes`.

[4] Amir Abboud, Vincent Cohen-Addad, and Hussein Houdrouge. Subquadratic high-dimensional hierarchical clustering. In *Advances in Neural Information Processing Systems*, pages 11580–11590, 2019.

[5] Nimar S Arora, Robert D Blumofe, and C Greg Plaxton. Thread scheduling for multiprogrammed multiprocessors. *Theory of Computing Systems (TOCS)*, 34(2):115–144, 2001.

[6] Martin Aumüller, Erik Bernhardsson, and Alexander Faithfull. Ann-benchmarks: A benchmarking tool for approximate nearest neighbor algorithms. In *International Conference on Similarity Search and Applications*, pages 34–49. Springer, 2017.

[7] We performed a similar comparison with the recently proposed ParChain framework for exact euclidean HAC [75]; here, ParHAC obtained an average of 39.3x speedup (end-to-end) in parallel over ParChain.

[7] Kevin Aydin, MohammadHossein Bateni, and Vahab Mirrokni. Distributed balanced partitioning via linear embedding. *Algorithms*, 12(8).

[8] MohammadHossein Bateni, Soheil Behnezhad, Mahsa Derakhshan, MohammadTaghi Hajiaghayi, Raimondas Kiveris, Silvio Lattanzi, and Vahab Mirrokni. Affinity clustering: Hierarchical clustering at scale. In *Advances in Neural Information Processing Systems (NeurIPS)*, pages 6864–6874, 2017.

[9] Jean-Paul Benzécri. Construction d'une classification ascendante hiérarchique par la recherche en chaîne des voisins réciproques. *Cahiers de l'analyse des données*, 7(2):209–218, 1982.

[10] Bonnie Berger, John Rompel, and Peter W. Shor. Efficient NC algorithms for set cover with applications to learning and geometry. *J. Computer and System Sciences*, 49(3):454–477, 1994.

[11] Guy E. Blelloch and Bruce M. Maggs. Algorithms and theory of computation handbook. chapter Parallel Algorithms. Chapman & Hall/CRC, 2010. ISBN 978-1-58488-820-8.

[12] Guy E. Blelloch, Richard Peng, and Kanat Tangwongsan. Linear-work greedy parallel approximate set cover and variants. In *ACM Symposium on Parallelism in Algorithms and Architectures (SPAA)*, pages 23–32, 2011.

[13] Guy E. Blelloch, Daniel Anderson, and Laxman Dhulipala. Parlaylib - a toolkit for parallel algorithms on shared-memory multicore machines. In *ACM Symposium on Parallelism in Algorithms and Architectures (SPAA)*, pages 507—-509, 2020.

[14] Guy E Blelloch, Jeremy T Fineman, Yan Gu, and Yihan Sun. Optimal parallel algorithms in the binary-forking model. In *ACM Symposium on Parallelism in Algorithms and Architectures (SPAA)*, pages 89–102, 2020.

[15] Guy E. Blelloch, Laxman Dhulipala, and Yihan Sun. Introduction to parallel algorithms. `http://www.cs.cmu.edu/~guyb/paralg/paralg/parallel.pdf`, 2021.

[16] RK Bock, A Chilingarian, M Gaug, F Hakl, Th Hengstebeck, M Jiřina, J Klaschka, E Kotrč, P Savickỳ, S Towers, et al. Methods for multidimensional event classification: a case study using images from a cherenkov gamma-ray telescope. *Nuclear Instruments and Methods in Physics Research Section A: Accelerators, Spectrometers, Detectors and Associated Equipment*, 516(2-3):511–528, 2004.

[17] Paolo Boldi and Sebastiano Vigna. The WebGraph framework I: Compression techniques. In *International World Wide Web Conference (WWW)*, pages 595–601, 2004.

[18] Otakar Borůvka. O jistém problému minimálním. *Práce Mor. Přírodověd. Spol. v Brně III*, 3: 37–58, 1926.

[19] Aydın Buluç, Henning Meyerhenke, Ilya Safro, Peter Sanders, and Christian Schulz. Recent advances in graph partitioning. *Algorithm engineering*, pages 117–158, 2016.

[20] Moses Charikar and Vaggos Chatziafratis. Approximate hierarchical clustering via sparsest cut and spreading metrics. In *ACM-SIAM Symposium on Discrete Algorithms (SODA)*, pages 841–854, 2017.

[21] Moses Charikar, Vaggos Chatziafratis, and Rad Niazadeh. Hierarchical clustering better than average-linkage. In *ACM-SIAM Symposium on Discrete Algorithms (SODA)*, pages 2291–2304, 2019.

[22] Evangelos Chatziafratis. *Hierarchical clustering with global objectives: Approximation algorithms and hardness results*. Stanford University, 2020.

[23] Michael Cochez and Hao Mou. Twister tries: Approximate hierarchical agglomerative clustering for average distance in linear time. In *ACM SIGMOD International Conference on Management of Data*, pages 505–517, 2015.

[24] Vincent Cohen-Addad, Varun Kanade, and Frederik Mallmann-Trenn. Hierarchical clustering beyond the worst-case. In *Advances in Neural Information Processing Systems*, volume 30, pages 6201–6209. Curran Associates, Inc., 2017.

[25] Vincent Cohen-Addad, Varun Kanade, Frederik Mallmann-Trenn, and Claire Mathieu. Hierarchical clustering: Objective functions and algorithms. *J. ACM*, 66(4), 2019.

[26] Thomas H. Cormen, Charles E. Leiserson, Ronald L. Rivest, and Clifford Stein. *Introduction to Algorithms (3. ed.)*. MIT Press, 2009.

[27] Sanjoy Dasgupta. A cost function for similarity-based hierarchical clustering. In *ACM Symposium on Theory of Computing (STOC)*, pages 118–127, 2016.

[28] Manoranjan Dash, Simona Petrutiu, and Peter Scheuermann. pPOP: Fast yet accurate parallel hierarchical clustering using partitioning. *Data Knowl. Eng.*, 61(3):563–578, 2007.

[29] Camil Demetrescu, Andrew Goldberg, and David Johnson. 9th dimacs implementation challenge: Shortest paths. http://www.dis.uniroma1.it/challenge9/, 2019.

[30] Laxman Dhulipala, Igor Kabiljo, Brian Karrer, Giuseppe Ottaviano, Sergey Pupyrev, and Alon Shalita. Compressing graphs and indexes with recursive graph bisection. In *ACM International Conference on Knowledge Discovery and Data Mining (KDD)*, pages 1535–1544, 2016.

[31] Laxman Dhulipala, Guy E. Blelloch, and Julian Shun. Julienne: A framework for parallel graph algorithms using work-efficient bucketing. In *ACM Symposium on Parallelism in Algorithms and Architectures (SPAA)*, pages 293–304, 2017.

[32] Laxman Dhulipala, Guy E. Blelloch, and Julian Shun. Theoretically efficient parallel graph algorithms can be fast and scalable. In *ACM Symposium on Parallelism in Algorithms and Architectures (SPAA)*, pages 293–304, 2018.

[33] Laxman Dhulipala, Guy E Blelloch, and Julian Shun. Low-latency graph streaming using compressed purely-functional trees. In *ACM SIGPLAN Conference on Programming Language Design and Implementation (PLDI)*, pages 918–934, 2019.

[34] Laxman Dhulipala, Changwan Hong, and Julian Shun. ConnectIt: A framework for static and incremental parallel graph connectivity algorithms. *Proc. VLDB Endow.*, 14(4):653–667, 2020.

[35] Laxman Dhulipala, Charlie McGuffey, Hongbo Kang, Yan Gu, Guy E Blelloch, Phillip B Gibbons, and Julian Shun. Sage: Parallel semi-asymmetric graph algorithms for NVRAMs. *Proc. VLDB Endow.*, 13(9):1598–1613, 2020.

[36] Laxman Dhulipala, Jessica Shi, Tom Tseng, Guy E. Blelloch, and Julian Shun. The graph based benchmark suite (GBBS). In *International Workshop on Graph Data Management Experiences and Systems (GRADES) and Network Data Analytics (NDA)*, pages 11:1–11:8, 2020.

[37] Laxman Dhulipala, David Eisenstat, Jakub Łącki, Vahab Mirrokni, and Jessica Shi. Hierarchical agglomerative graph clustering in nearly-linear time. In *International Conference on Machine Learning (ICML)*, pages 2676–2686, 2021.

[38] Laxman Dhulipala, Guy E Blelloch, Yan Gu, and Yihan Sun. PaC-trees: Supporting parallel and compressed purely-functional collections. In *ACM SIGPLAN Conference on Programming Language Design and Implementation (PLDI)*, 2022.

[39] Jordi Fonollosa, Sadique Sheik, Ramón Huerta, and Santiago Marco. Reservoir computing compensates slow response of chemosensor arrays exposed to fast varying gas concentrations in continuous monitoring. *Sensors and Actuators B: Chemical*, 215:618–629, 2015.

[40] P. Franti, O. Virmajoki, and V. Hautamaki. Fast agglomerative clustering using a k-nearest neighbor graph. *IEEE Transactions on Pattern Analysis and Machine Intelligence*, 28(11): 1875–1881, 2006.

[41] Sudipto Guha, Rajeev Rastogi, and Kyuseok Shim. Rock: A robust clustering algorithm for categorical attributes. In *Proceedings of the International Conference on Data Engineering*, pages 512–521, USA, 1999.

[42] Katherine A. Heller and Zoubin Ghahramani. Bayesian hierarchical clustering. In *International Conference on Machine Learning (ICML)*, pages 297–304, 2005.

[43] Changwan Hong, Laxman Dhulipala, and Julian Shun. Exploring the design space of static and incremental graph connectivity algorithms on gpus. In *International Conference on Parallel Architectures and Compilation Techniques (PACT)*, pages 55–69, 2020.

[44] Suhas Jayaram Subramanya, Fnu Devvrit, Harsha Vardhan Simhadri, Ravishankar Krishnawamy, and Rohan Kadekodi. DiskANN: Fast accurate billion-point nearest neighbor search on a single node. *Advances in Neural Information Processing Systems*, 32, 2019.

[45] Yongkweon Jeon and Sungroh Yoon. Multi-threaded hierarchical clustering by parallel nearest-neighbor chaining. *IEEE Trans. Parallel Distributed Syst.*, 26(9):2534–2548, 2015.

[46] Igor Kabiljo, Brian Karrer, Mayank Pundir, Sergey Pupyrev, and Alon Shalita. Social hash partitioner: A scalable distributed hypergraph partitioner. *Proc. VLDB Endow.*, 10(11):1418–1429, 2017.

[47] George Karypis, Eui-Hong (Sam) Han, and Vipin Kumar. Chameleon: Hierarchical clustering using dynamic modeling. *Computer*, 32(8):68–75, August 1999.

[48] Benjamin King. Step-wise clustering procedures. *Journal of the American Statistical Association*, 69:86–101, 1967.

[49] Haewoon Kwak, Changhyun Lee, Hosung Park, and Sue Moon. What is twitter, a social network or a news media? In *International World Wide Web Conference (WWW)*, pages 591–600, 2010.

[50] G. N. Lance and W. T. Williams. A general theory of classificatory sorting strategies 1. Hierarchical systems. *Computer Journal*, 9(4):373–380, February 1967.

[51] Jure Leskovec and Andrej Krevl. SNAP Datasets: Stanford large network dataset collection, 2014.

[52] Christopher D Manning, Prabhakar Raghavan, and Hinrich Schütze. *Introduction to Information Retrieval*. Cambridge University Press, 2008.

[53] Robert Meusel, Sebastiano Vigna, Oliver Lehmberg, and Christian Bizer. The graph structure in the web–analyzed on different aggregation levels. *The Journal of Web Science*, 1(1):33–47, 2015.

[54] Nicholas Monath, Avinava Dubey, Guru Guruganesh, Manzil Zaheer, Amr Ahmed, Andrew McCallum, Gokhan Mergen, Marc Najork, Mert Terzihan, Bryon Tjanaka, et al. Scalable agglomerative clustering. In *ACM International Conference on Knowledge Discovery and Data Mining (KDD)*, pages 1245–1255, 2021.

[55] Benjamin Moseley and Joshua R. Wang. Approximation bounds for hierarchical clustering: Average linkage, bisecting k-means, and local search. In *Advances in Neural Information Processing Systems*, pages 3094–3103, 2017.

[56] Benjamin Moseley, Kefu Lu, Silvio Lattanzi, and Thomas Lavastida. A framework for parallelizing hierarchical clustering methods. In *ECML PKDD 2019*, 2019.

[57] Fionn Murtagh and Pedro Contreras. Algorithms for hierarchical clustering: an overview. *Wiley Interdisciplinary Reviews: Data Mining and Knowledge Discovery*, 2(1):86–97, 2012.

[58] Daniel Müllner. fastcluster: Fast hierarchical, agglomerative clustering routines for r and python. *Journal of Statistical Software, Articles*, 53(9):1–18, 2013.

[59] Clark F. Olson. Parallel algorithms for hierarchical clustering. *Parallel Comput.*, 21(8):1313–1325, 1995.

[60] C. A. Phillips. Parallel graph contraction. In *ACM Symposium on Parallelism in Algorithms and Architectures (SPAA)*, pages 148–157, 1989.

[61] Sanguthevar Rajasekaran. Efficient parallel hierarchical clustering algorithms. *IEEE Transactions on Parallel and Distributed Systems*, 16(6):497–502, 2005.

[62] J. Reif. Optimal parallel algorithms for integer sorting and graph connectivity. Technical Report TR-08-85, Harvard University, 1985.

[63] Aurko Roy and Sebastian Pokutta. Hierarchical clustering via spreading metrics. In *Advances in Neural Information Processing Systems (NIPS)*, volume 29, pages 2316–2324. Curran Associates, Inc., 2016.

[64] Jianyin Shao, Stephen W. Tanner, Nephi Thompson, and Thomas E. Cheatham. Clustering molecular dynamics trajectories: 1. Characterizing the performance of different clustering algorithms. *Journal of Chemical Theory and Computation*, 3(6):2312–2334, 2007.

[65] Jessica Shi, Laxman Dhulipala, David Eisenstat, Jakub Łăcki, and Vahab Mirrokni. Scalable community detection via parallel correlation clustering. *Proc. VLDB Endow.*, 14(11):2305–2313, 2021.

[66] Jessica Shi, Laxman Dhulipala, and Julian Shun. Parallel clique counting and peeling algorithms. In *SIAM Conference on Applied and Computational Discrete Algorithms (ACDA21)*, pages 135–146. SIAM, 2021.

[67] Julian Shun and Guy E Blelloch. Phase-concurrent hash tables for determinism. In *ACM Symposium on Parallelism in Algorithms and Architectures (SPAA)*, pages 96–107, 2014.

[68] Julian Shun, Laxman Dhulipala, and Guy E. Blelloch. A simple and practical linear-work parallel algorithm for connectivity. In *ACM Symposium on Parallelism in Algorithms and Architectures (SPAA)*, pages 143–153, 2014.

[69] Julian Shun, Laxman Dhulipala, and Guy E. Blelloch. Smaller and faster: Parallel processing of compressed graphs with Ligra+. In *Data Compression Conference (DCC)*, pages 403–412, 2015.

[70] Peter H.A. Sneath and Robert R. Sokal. *Numerical Taxonomy: The Principles and Practice of Numerical Classification*. W.H. Freeman, San Francisco, 1973. ISBN 0 7167 0697 0.

[71] Baris Sumengen, Anand Rajagopalan, Gui Citovsky, David Simcha, Olivier Bachem, Pradipta Mitra, Sam Blasiak, Mason Liang, and Sanjiv Kumar. Scaling hierarchical agglomerative clustering to billion-sized datasets. *CoRR*, abs/2105.11653, 2021.

[72] The SciPy community. scipy.cluster.hierarchy.linkage. URL `https://docs.scipy.org/doc/scipy/reference/generated/scipy.cluster.hierarchy.linkage.html`. [Online; accessed 1-May-2022].

[73] Tom Tseng, Laxman Dhulipala, and Julian Shun. Parallel batch-dynamic minimum spanning forest and the efficiency of dynamic agglomerative graph clustering. *arXiv preprint arXiv:2205.04956*, 2022.

[74] Joe H. Ward. Hierarchical grouping to optimize an objective function. *Journal of the American Statistical Association*, 58(301):236–244, 1963. ISSN 01621459.

[75] Shangdi Yu, Yiqiu Wang, Yan Gu, Laxman Dhulipala, and Julian Shun. Parchain: A framework for parallel hierarchical agglomerative clustering using nearest-neighbor chain. *Proc. VLDB Endow.*, 15(2):285–298, 2021.

[76] Yu Zheng, Like Liu, Longhao Wang, and Xing Xie. Learning transportation mode from raw GPS data for geographic applications on the web. In *International Conference on World Wide Web*, pages 247–256, 2008.

A Missing Details and Proofs

We denote the degree of vertex v by $deg(v)$ and use $\mathsf{Cut}(X, Y)$ to denote the set of edges between two sets of vertices X and Y.

In this paper we focus on the *average-linkage measure* (sometimes also called *unweighted average-linkage* or *UPGMA-linkage*), which assumes that the similarity between two clusters (X, Y) is equal to $\sum_{(x,y)\in\mathsf{Cut}(X,Y)} w(x, y)/(|X| \cdot |Y|)$, that is the total weight of edges between X and Y, divided by the maximum number of possible edges between the clusters. A less common variant of average-linkage is *weighted average-linkage (WPGMA-linkage)*. For this measure, the similarity between two clusters depends not only on the current clustering, but also on the sequence of merges that created it. In particular, if a cluster Z is created by merging clusters X and Y, the similarity of the edge between Z and a neighboring cluster U is $\frac{\mathcal{W}(X,U)+\mathcal{W}(Y,U)}{2}$ if both edges (X, U) and (Y, U) exist before the merge, and otherwise just the weight of the single existing edge. We stress that *unweighted* and *weighted* in the linkage measure names refer to the linkage methods. In both cases, throughout this paper we consider graphs with arbitrary non-negative edge weights.

A linkage measure is *reducible* [9], if for any three clusters X, Y, Z, it holds that $\mathcal{W}(X \cup Y, Z) \leq \max(\mathcal{W}(X, Z), \mathcal{W}(Y, Z))$. We note that both average-linkage and weighted average-linkage are reducible [9].

A.1 Sequential HAC

We start by reviewing the existing exact and $(1 + \epsilon)$-approximate sequential HAC algorithms which are two baselines that we compare against, and also the starting point for our theoretical results.

Exact Average-Linkage. A challenge in implementing the average-linkage HAC algorithm is to efficiently maintain edge weights in the graph as vertices (clusters) are merged. Since the average-linkage formula includes the cluster sizes of both endpoints of a (u, v) edge when computing the weight of the edge, an algorithm which eagerly maintains the correct weights of all edges in the graph must update *all* of the edge weights incident to a newly merged cluster. Unfortunately, even for sparse graphs with $O(n)$ edges, one can show that such an eager approach requires $\Omega(n^2)$ time.

It was recently shown [37] that the exact average-linkage HAC algorithm can be implemented in $\tilde{O}(n\sqrt{m})$ time, using the classic nearest-neighbor chain technique [9, 57] in conjunction with a low-outdegree orientation data structure.

Approximate Average-Linkage (SeqHAC). Our parallel algorithm is inspired by a recent sequential approximate average-linkage HAC algorithm which we refer to as SeqHAC [37], which runs in near-linear time. The sequential algorithm uses a lazy strategy to avoid updating the weights of all edges incident to each merged vertex. Instead of exactly maintaining the weight of each edge, the algorithm uses the observation that the weights of edges incident to a vertex do not need to be updated every time the cluster represented by this vertex grows. Namely, if we allow an $(1 + \epsilon)^2$-approximate algorithm, the weights of edges incident to a vertex do not need to be updated until the cluster-size of this vertex grows by a multiplicative $(1 + \epsilon)$ factor. (The approximation ratio of the algorithm is squared, since the clusters represented by *both* endpoints of an edge may grow by a $(1 + \epsilon)$ factor before its weight is updated.) As this can happen at most $O(\log_{1+\epsilon} n)$ times, for a constant ϵ, the overall number of edge weight updates is $\tilde{O}(m)$.

The approximate algorithm adapts the folklore *heap-based* approach [57], originally designed for an exact setting to the approximate setting. Specifically, the approximate algorithm maintains a heap keyed by the vertices, where the value assigned to a vertex is its current highest-weight incident edge (whose weight is correct up to a $(1 + \epsilon)^2$ factor). In each iteration, the highest-weight edge is chosen from the heap and its endpoints are merged. By setting parameters appropriately one can ensure that the resulting algorithm is $(1 + \epsilon)$-approximate.

A.2 Motivating ParHAC

Recall that our approach is based on *geometric layering*, where we group the edges based on their weights and process all edges within the same layer in parallel. Let $\mathcal{W}_{\max}$ and $\mathcal{W}_{\min}$ be the maximum-weight and minimum-weight in the graph, respectively. In the geometric layering scheme,

the i-th layer contains all edges with weight between $((1+\epsilon)^{-(i+1)} \cdot \mathcal{W}_{\max}, (1+\epsilon)^{-i} \cdot \mathcal{W}_{\max}]$. The layering algorithm then processes these layers one-by-one, starting with the heaviest-weight layer. An ***active vertex*** is a vertex that has edges in the layer currently being processed by the algorithm. Under the standard assumption that the ***aspect-ratio*** of the graph is polynomially bounded, that is $\mathcal{A} = \mathcal{W}_{\max}/\mathcal{W}_{\min} = O(\mathsf{poly}(n))$, we can show that the maximum number of layers processed by the algorithm is $O(\log n)$ for any constant ϵ. We note that on the real-world datasets evaluated in this paper, which include both graphs derived from real-world pointsets, and real-world graphs, the aspect ratio is at most 1000, and that all existing HAC approximation algorithms make similar assumptions on the aspect ratio [4, 37]. The key challenge for a parallel approximation algorithm based on this paradigm is that it must process all of the elements within each layer in $\mathsf{polylog}(n)$ rounds, while ensuring that it does not violate the $(1+\epsilon)$ approximation requirements.

Natural Approaches: Spanning Forest and Affinity. A natural idea is to compute a spanning forest induced by the edges within the current layer, and to merge together all vertices in each tree in the forest. Using this approach, all edges within the current layer can be processed in a single spanning-forest step. Furthermore, after applying these merges all remaining edges in the graph fall into layers of smaller weight. Using a work-efficient spanning forest algorithm, the overall work and depth of this approach will be $\tilde{O}(m)$ and $O(\mathsf{polylog}(n))$, respectively [68].

A similar idea is used in the *Affinity Clustering* algorithm of Bateni et al. [8]. In this algorithm, each vertex marks its highest-weight incident edge, and the sets of vertices to be merged are the connected components of the graph formed by the marked edges. It is easy to see that this approach yields a $\tilde{O}(m)$ work and $O(\mathsf{polylog}(n))$ depth algorithm in the geometric layering scheme.

Unfortunately, both of these natural approaches fail to yield $(1+\epsilon)$-approximate algorithms because they both choose "locally good" edges to merge without taking into account how the similarities of these edges change as they are mapped to binary merges in the dendrogram. For example, if the input graph is a path consisting of edges of the same weight, the spanning forest approach would merge all of the vertices together in one step. At the same time it is easy to see that for $\epsilon < 1/2$ an $(1+\epsilon)$-approximate algorithm, within a single layer, must merge sets of vertices of size at most 2.

Our Approach: Capacitated Random Mate. Our approach is inspired by the classic random-mate technique [11] when processing each layer, but requires a careful modification to yield good approximation guarantees. Our algorithm starts by first randomly coloring the active vertices red and blue with equal probability. Directly applying the random-mate approach (e.g., as applied in the parallel connectivity algorithms of Reif [62] and Phillips [60]) would suggest merging all blue vertices into an arbitrary red neighbor. The number of edges in the layer decreases by a constant factor in expectation, thus yielding the desired work and depth bounds. Unfortunately, this approach does not yield good approximation guarantees for the same reason that the spanning forest and affinity approaches fail to do so. The issue is that the size of a red cluster can become too large, causing the similarity of a merged edge to be much smaller than $W_{\max}/(1+\epsilon)$, where $W_{\max}$ is the *current largest edge weight*.

Our *capacitated random-mate* approach fixes this issue with the classic random-mate strategy by processing each layer in multiple *rounds* and enforcing vertex-capacities for the red vertices in each round. These capacities ensure that the sizes of clusters represented by red vertices increase by at most a $(1+\epsilon)$ factor within a round. As a result, the weight of each edge incident to a red vertex may only decrease by a $(1+\epsilon)$ factor.

Specifically, consider a red vertex v representing a cluster C. Assume that at the beginning of a round all edge weights in the graph are computed exactly and the size of the cluster C is c_0. Within the round, vertex v only accepts a merge proposal from a neighboring blue vertex if the total size of the cluster C, including the growth incurred by previous proposals accepted within this round, is smaller than $(1+\epsilon)c_0$. This approach ensures that the weight of any merged edge is close to $W_{\max}$, and thus lets us argue that our algorithm is $(1+\epsilon)$-approximate. However, using this capacitated approach complicates the analysis of the round-complexity of our algorithm, making it more challenging to bound the overall work and depth. Our main theoretical contribution is to show that the capacitated approach results in a near-linear work and poly-logarithmic depth algorithm (ParHAC) that achieves a $(1+\epsilon)$-approximation for any $\epsilon > 0$.

Algorithm 2 ParHAC($G = (V, E, w), \epsilon$)

Input: Similarity graph G, $\epsilon > 0$.
Ensure: $(1 + \epsilon)$-approximate dendrogram for unweighted average-linkage HAC.
1: Let D be initialized to the identity clustering.
2: **while** $|E| > 0$ **do**
3: Let $W_{\max}$ be the current maximum-weight edge in the graph.
4: Call ParHAC-CONTRACTLAYER$\big(G, (1 + \epsilon)^{-1} \cdot W_{\max}, \epsilon, D\big)$.
5: **return** D

A.3 Missing Proofs

Algorithm 2 shows the layer-based ParHAC algorithm. Next, we present the missing proofs for the work-depth and approximation analysis of the algorithm.

Lemma A.1. *Assuming that the aspect-ratio of the graph, $\mathcal{A} = O(\mathsf{poly}(n))$, the number of layer-contraction phases is $O(\log n)$.*

Proof. Since the unweighted average-linkage function is reducible, the largest weight can only decrease over the course of the algorithm. Furthermore, the smallest weight that the algorithm can encounter using the unweighted average-linkage function is proportional to $O(\mathcal{W}_{\min}/n^2)$. Thus the weight range that the algorithm runs over is $\mathcal{W}_{\max}/(\mathcal{W}_{\min}/n^2) = O(\mathsf{poly}(n))$, and only $O(\log n)$ layers are required to represent every weight in this weight range. □

Lemma 2.1. *Consider an arbitrary blue vertex b within an inner round. Within this round either (a) a constant factor of edges incident to b are deleted, or (b) with constant probability b is merged into one of its red neighbors.*

Proof. Fix the random priority π_b for each $b \in B$. We show that the lemma follows for *any* set of distinct priorities, not necessarily random ones. It is easy to see that our algorithm is equivalent to processing the blue vertices in the order of their priorities and deciding for each of them whether it merges to a red neighbor. We say that a red vertex is *saturated* if its size has increased by more than $(1 + \epsilon)$ factor since the beginning of the outer round. Note that each saturated red vertex is removed at the end of the inner iteration. Now, consider a blue vertex b. If more than half of red neighbors of b are saturated, we are in case (a). Otherwise, with constant probability b chooses a non-saturated red neighbor and can merge with it. □

Lemma A.2. *There are at most $O(\log n)$ inner rounds within each outer round with high probability.*

Proof. Fix a blue vertex b. There can be at most $O(\log n)$ inner rounds when the vertex satisfies case (a) of Lemma 2.1, and at most $O(\log n)$ times (with high probability) when it satisfies case (b). After that, the vertex is either merged into its red neighbor or becomes isolated. In both cases, all incident edges are removed. □

Lemma 2.2. *The number of outer rounds in a call to Algorithm 1 is $O(\log n)$ with high probability.*

Proof. Consider the **while** loop in Line 6. We first prove the following claim: for each edge e of the graph G_c at the beginning of the loop, either (a) the endpoints of e are merged together, or (b) the weight of e drops below T_L, or (c) an endpoint of e increases its size by a factor of $(1 + \epsilon)$.

To prove this fact, we observe that when the loop terminates, all edges of G_c have been removed. Clearly, an edge can be removed when its endpoints are merged together or when its weight drops below T_L, which corresponds to cases (a) and (b). There are two more ways of removing an edge. First, an edge can be removed on Line 16 when its red endpoint grows by a factor of $(1 + \epsilon)$, which leads to case (c). Second, the edge can be removed when it connects two red vertices. This can only happen as a result of a blue vertex merging into a red vertex. However, since for each edge in G_c the red endpoint has size not smaller than the blue one, whenever a blue vertex merges into a red one, the size of its cluster doubles. This finishes the proof of the claim.

From this claim, we immediately conclude that for a fixed layer, any edge e of G can participate in at most $O(\log n)$ inner rounds, as each endpoint of e can increase its size at most $O(\log n)$ times. Since within an outer round, e is included in G_c with constant probability, we conclude there can be at most $O(\log n)$ outer rounds with high probability. □

Lemma A.3. *Each outer round can be implemented in $O(m \log n + n \log^2 n)$ expected work and $O(\log^2 n)$ depth with high probability.*

Proof. Computing G_c (Line 5) and updating G and G_c within (Line 13) can be done in $O(m)$ work and $O(\log n)$ depth using standard parallel primitives such as prefix-sum and filter [15]. Using a parallel comparison sort, Line 9 costs $O(n \log n)$ work and $O(\log n)$ depth [15]. The remaining steps can be implemented in $O(n)$ work and $O(\log n)$ depth using standard parallel primitives. Combining the work-depth analysis with the fact that there are $O(\log n)$ inner rounds *whp* by Lemma A.2 completes the proof. □

The work-and depth component of Theorem 2.3 follows immediately from Lemma A.3, and due to the fact that there are $O(\log n)$ outer rounds (Lemma 2.2), and $O(\log n)$ layers overall (Lemma A.1). We prove the final part of Theorem 2.3 by showing that ParHAC is a good approximation to sequential average-linkage HAC.

Theorem A.4. ParHAC *is an $(1+\epsilon)$-approximate average-linkage HAC algorithm.*

Proof. Let $1+\delta$ be the approximation parameter used internally in the algorithm, which we will set shortly as a function of ϵ. Consider the merges performed within an inner round in the algorithm. In the algorithm these merges only occur between blue vertices and their red neighbors that they are connected to with an edge with weight at least T_L (the lower layer-threshold). At the start of a layer-contraction phase the maximum similarity in the graph is $W_{\max}$ and we have by construction that $(1+\delta)^{-1} W_{\max} \leq T_L$. Furthermore, since the average-linkage function is reducible the maximum similarity in the graph throughout the rest of this layer-contraction phase is always upper-bounded by $W_{\max}$.

Consider the merges done within one inner round of the algorithm. We know that for each red vertex r that participates in merges in this inner round, its cluster size never exceeds $(1+\delta)S_I(r)$ where $S_I(r)$ is the cluster-size of r at the start of the outer round. Furthermore, since we maintain the exact weights of all edges in both G and G_c after every inner round finishes (in Line 13), we know that the weight of each (b_i, r) edge for each blue vertex b_i merging into r in this round is at least T_L. Therefore, the smallest value this weight can attain in a merge is $T_L/(1+\delta)$, which is lower-bounded by $(1+\delta)^{-2} W_{\max}$. Therefore, our approach yields a $(1+\delta)^{-2}$-approximate algorithm. Now, for $\epsilon \leq 1$ we set $\delta = \epsilon/3$, and for $\epsilon > 1$, we set $\delta = \sqrt{\epsilon}/3$. Thus, we obtain an $(1+\epsilon)$-approximate algorithm for average-linkage HAC for any $\epsilon > 0$. □

B Parallel Hardness of Graph-Based HAC

We show hardness results for the graph-based HAC problem under two fundamental linkage measures.

B.1 Hardness for Graph-Based HAC using Weighted Average-Linkage

We start by presenting our lower bound for weighted average-linkage measure as our lower bound for average-linkage builds on it. The problem is in P, and so we show P-hardness to show the P-completeness result. We do this by providing an NC reduction from the P-complete monotone circuit-value problem (monotone CVP).

In monotone CVP, we are given circuit consisting of gates, that has n input variables $x_1, \ldots, x_n$, along with an assignment of truth values to each of the initial variables. The literals x_i and $\bar{x_i}$ appear as initial truth-values set based on the truth-value of x_i. The circuit is monotone, so the gates consist of only AND and OR gates.

Since the topological ordering of a DAG can be computed in NC, we can assume that the circuit consists of t gates $g_1, \ldots, g_t$ where each of $g_1, \ldots, g_{2n}$ corresponds to one input literal or its negation, and for $i > 2n$, gate g_i has exactly two inputs, which are gates with indices less than i.

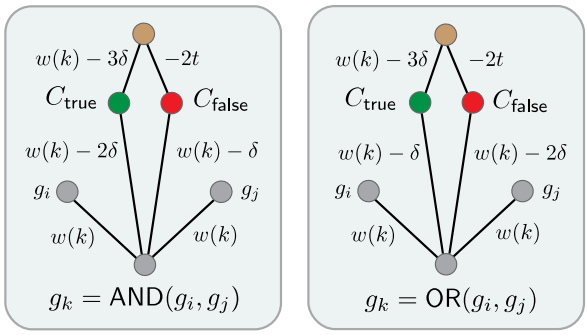


Figure 4: This figure illustrates the gadgets used in the reduction from the monotone circuit value problem to show that graph-based HAC using weighted average-linkage is P-complete.

Construction. The reduction builds a graph $H = (V', E')$ with $2t - 2n + 2$ vertices, where $V' = \{g_1, \ldots, g_t, C_{\mathsf{true}}, C_{\mathsf{false}}, d_{2n+1}, d_{2n+2}, \ldots, d_t\}$ illustrated in Figure 4. The high-level idea is to ensure that running graph-based HAC on H results in gates evaluating to true merging into C_{true} and gates evaluating to false merging into C_{false}. The only role of vertices $d_{2n+1}, d_{2n+2}, \ldots, d_t$ is to prevent C_{true} and C_{false} from merging with each other until the final merge. To this end, each of the vertices d_k will have a positive-weight edge to C_{true} and a negative-weight edge to C_{false}.

Note that the construction can be easily modified not to use negative weights, since in the case of weighted average-linkage increasing all edge weights by the same amount does not affect the course of the algorithm.

The construction is entirely local and can thus be easily parallelized using standard parallel primitives such as prefix-sums. The graph we define adds a gadget for each gate, which is defined using $w(i) := t - i$, and a constant $\delta \in (0, 1/4)$.

The graph H is constructed by adding the following set of edges. For each $k = 1, \ldots, t$:

1. If $k \leq 2n$, we add an edge of weight $w(0)$ between g_k and C_{true} or C_{false}, depending of the value of the literal g_k.
2. Assume $k > 2n$ and $g_k = \mathsf{AND}(g_i, g_j)$. We add the following edges: $\{(g_k, C_{\mathsf{true}}, w(k) - 2\delta), (g_k, C_{\mathsf{false}}, w(k) - \delta), (g_k, g_i, w(k)), (g_k, g_j, w(k)), (d_k, C_{\mathsf{true}}, w(k) - 3\delta), (d_k, C_{\mathsf{false}}, -2t)\}$.
3. Assume $k > 2n$ and $g_k = \mathsf{AND}(g_i, g_j)$. We add the following edges: $\{(g_k, C_{\mathsf{true}}, w(k) - \delta), (g_k, C_{\mathsf{false}}, w(k) - 2\delta), (g_k, g_i, w(k)), (g_k, g_j, w(k)), (d_k, C_{\mathsf{true}}, w(k) - 3\delta), (d_k, C_{\mathsf{false}}, -2t)\}$.

Finally, we add an edge between C_{true} and C_{false} of weight $-t$. An illustration of the resulting gadgets built from g_k for AND and OR gates is shown in Figure 4. We first show that the gadgets are processed in the order of their indices.

Lemma B.1. *Consider running the graph-based HAC algorithm with weighted average-linkage on H. For any $k \geq 2n$, the algorithm begins by merging gates $g_1, \ldots, g_k$ and $d_{2n+1}, \ldots, d_k$ into C_{true} or C_{false}, before merging any gates with indices larger than k. Moreover, once all gates of indices up to k have been merged, the weight of the edge between C_{true} and C_{false} is at most $-t$.*

Proof. We prove the claim by induction on k. To show the base case, we need to show that the algorithm begins by merging the gates corresponding to literals to either C_{true} or C_{false}.

Observe that $w(0)$, the edge weight used for connecting literals to C_{true} or C_{false}, is the largest edge weight in the graph. Moreover, each merge of a literal gate reduces by 1 the number of edges of weight at least $w(0)$, so the algorithm indeed begins by merging gates $g_1, \ldots, g_{2n}$ into C_{true} or C_{false}.

Consider now $k > 2n$ and assume the algorithm has merged $g_1, \ldots, g_{k-1}$ and $d_{2n+1}, \ldots, d_{k-1}$ into C_{true} and C_{false}. Hence, the remaining set of vertices are $g_k, \ldots, g_t, d_k, \ldots, d_t, C_{\mathsf{true}}$, and C_{false}.

Let us look at the set of edge weights in the remaining graph.

- For any d_j, where $j \geq k$, clearly the incident edges still have weights $w(j) - 3\delta$ and $-4t$.
- For any g_j, where $j \geq k$, by induction hypothesis, g_j has not yet participated in any merges. In the original graph the edges incident to g_j connect g_j to
  1. its inputs (weight $w(j)$),
  2. C_{true} and C_{false} (weight at least $w(j) - 2\delta$),
  3. gates with indices larger than j (of weight at most $w(j) - 1$).

  By the induction hypothesis, the only change that may have happened to the set of edges incident to g_j is that edges of type 1 above *may* have been merged with edges of type 2. Still, g_j has an incident edge of weight belonging to $(w(j) - 2\delta, w(j)]$.
- In addition, there is an edge between C_{true} and C_{false} of negative weight.

From the definition of $w(\cdot)$ it follows that the only edges of weight more than $w(k) - 1$ are incident to g_k and d_k. Moreover, the highest weight edge is incident to g_k. Since both inputs to g_k have been already merged into C_{true} or C_{false}, it follows that g_k merges into one of them as well. After that, d_k merges into C_{true}.

Before these two steps, the edge between C_{true} and C_{false} had weight of at most $-t$. Since $(w(k) - t)/2 \leq 0$, after the first merge, the weight between C_{true} and C_{false} remains negative. Denote it by x. After d_k is merged into C_{true}, the weight of the edge between C_{true} and C_{false} is $(x - 2t)/2 \leq -2t/2 = -t$. □

Lemma B.2. *Consider running graph-based HAC algorithm with weighted average-linkage on H until no edges of nonnegative weight remain. Then, the algorithm produces exactly two clusters, where one of them contains C_{true} and vertices corresponding to gates that evaluate to* true *and the other one contains C_{false} and all vertices corresponding to gates that evaluate to* false*.*

Proof. We show that gates $g_1, \ldots, g_k$ are correctly merged into C_{true} or C_{false} using an induction on k. For $k \leq 2n$ this follows directly from the construction and Lemma B.1.

Now assume $k > 2n$. We use Lemma B.1 and look at the point where g_k is merged for the first time. At this point, we know that the inputs to g_k have been (correctly) merged into C_{true} or C_{false}.

The proof is a case-by-case analysis, depending on the gate type and the values of the inputs. For example, if $g_k = \mathsf{AND}(g_i, g_j)$, and $g_i = g_j = \mathsf{true}$, we have that the updated weight of $(g_k, C_{\mathsf{true}}) = 1 - \delta/2$, and the weight of $(g_k, C_{\mathsf{false}}) = 1 - \delta$, and therefore g_k is correctly merged with C_{true}. On the other hand, if one or both of $\{g_i, g_j\} = \mathsf{false}$, then the updated weight of $(g_k, C_{\mathsf{true}}) \leq 1 - \delta$, and the weight of $(g_k, C_{\mathsf{false}}) \geq 1 - \delta/2$, ensuring that g_k is correctly merged with C_{false}. It is easy to check the other cases similarly.

It follows from Lemma B.1 that the clusters containing C_{true} and C_{false} are never merged with each other. The Lemma follows. □

This immediately implies the following.

Theorem B.3. *Graph-based HAC using weighted average-linkage is* P*-complete.*

B.2 Hardness for Graph-Based HAC using Average-Linkage

Our reduction for average-linkage is similar to the reduction for weighted average-linkage, but requires additional steps to handle how average-linkage adjusts the weight of an edge between two clusters based on their respective sizes. [8]

As before, our reduction starts from the monotone CVP problem, and the idea is to have HAC simulate the execution of the circuit so that gates evaluating to true (false) are merged to C_{true} (C_{false}).

One of the main problems to deal with is that the weight of an edge between two clusters U and V in average-linkage is equal to the sum of the weights crossing the cut from U to V normalized by the

[8] Note that average-linkage is *not* a special case of weighted average-linkage measure. See the start of Appendix A for the definitions.

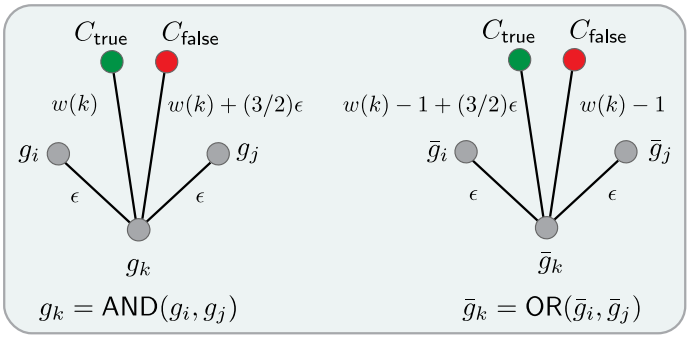


Figure 5: Gadgets used in the reduction from the monotone circuit value problem to show that graph-based HAC using average-linkage is P-complete.

product $|U| \cdot |V|$. The challenge is that we do not know (without running the algorithm) what the size of C_{true} or C_{false} will be at some intermediate step in the algorithm, since these sizes depend on the number of gates that evaluate to true and false respectively.

To fix this problem, we add *two vertices per gate* corresponding to g_i and $\bar{g}_i$ and ensure that if g_i merges to C_{true}, $\bar{g}_i$ merges to C_{false}. In addition, we need to assure that C_{true} and C_{false} do not merge with each other. To this end, we ensure that the graph-based HAC algorithm starts by increasing the clusters of both C_{true} and C_{false} to a large size, which makes them harder to merge with each other.

Construction. As in the case of weighted average linkage, we can assume that the circuit consists of t gates $g_1, \ldots, g_t$ where each of $g_1, \ldots, g_{2n}$ corresponds to one input literal or its negation, and for $i > 2n$, gate g_i has exactly two inputs, which are gates with indices less than i. The reduction builds a graph $H = (V', E')$, which initially has two special vertices, C_{true} and C_{false}. In the description we use $w(k) := 4t - 2k$ and $\epsilon = 1/100$.

First, we add $(1/\epsilon - 3) \cdot t$ dummy vertices, and connect half of them to C_{true} and half to C_{false} using edges of weight t^3.

Then, we add $2n$ vertices corresponding to the literals, and connect each of them to either C_{true} or C_{false}, depending on the literal value, also with an edge of weight t^3. These high weight edges ensure that the graph-based HAC algorithm proceeds by merging the dummy vertices and literal vertices to C_{true} or C_{false}.

Finally, we add $2(t - 2n)$ vertices corresponding to the gates. For a fixed i ($2n < i \leq t$), we add two vertices g_i and $\bar{g}_i$ corresponding to gate g_i in the circuit.

1. For $g_k = \mathsf{AND}(g_i, g_j)$, create a vertex g_k with edges:
   $\{(g_k, C_{\mathsf{true}}, w(k)), (g_k, C_{\mathsf{false}}, w(k) + (3/2)\epsilon)\}$ and
   $\{(g_k, g_i, \epsilon), (g_k, g_j, \epsilon))\}$.
2. For $\bar{g}_k = \mathsf{OR}(\bar{g}_i, \bar{g}_j)$, create a vertex $\bar{g}_k$ with edges:
   $\{(\bar{g}_k, C_{\mathsf{true}}, w(k) - 1 + (3/2)\epsilon), (\bar{g}_k, C_{\mathsf{false}}, w(k) - 1)\}$ and
   $\{(\bar{g}_k, \bar{g}_i, \epsilon), (\bar{g}_k, \bar{g}_j, \epsilon)\}$.

The construction for $g_k = \mathsf{AND}(g_i, g_j)$ swaps g_k and $\bar{g_k}$ in the descriptions above. Induction over the merge steps, performing case analysis on the truth values of the inputs to each gate, similar to our proof for weighted average-linkage yields the following theorem.

Theorem B.4. *Graph-based HAC using average-linkage is* P*-complete.*

Proof. Let a merge step of the graph-based HAC algorithm be two consecutive merges that it performs, and call the internal merges sub-merges. The proof shows by induction on the merge steps that the next merge merges the vertices g and $\bar{g}$, and that the merge correctly simulates the circuit logic for g and $\bar{g}$.

Suppose in the k-th step that some vertex $g_{k'}$, with $k' > k$ is merged instead of g_k (the proof is essentially identical for $\bar{g}_k$). We consider two cases. In the first case, suppose the merge is between $g_{k'}$ and either C_{true} or C_{false}. Denote the weights of C_{true} and C_{false} by r. The weight of the edge

between g_k and C_{true} or C_{false} is at least $w(k)/r$ and the weight of any edge incident to $g_{k'}$ is at most $(w(k') + (5/2)\epsilon)/r < w(k)/r$, a contradiction.

In the second case, suppose the merge is between $g_{k'}$ and one of its inputs, g_j, which clearly uses an edge of weight at most ϵ. To argue that this cannot happen, we show that the linkage similarity of g_k to both C_{true} and C_{false} is greater than ϵ. Indeed, the cluster size of both C_{true} and C_{false} is at most $1 + t(1/\epsilon - 3) + 2t < t/\epsilon$. Hence, the weight of an edge from g_k to any of these clusters is at least $(w(k) - 1)/(t/\epsilon) \leq (w(t) - 1)/(t/\epsilon) = (4t - 2t - 1)/(t/\epsilon) > \epsilon$.

Finally, we also show that C_{true} and C_{false} do not merge with each other. Observe that the sizes of both these clusters are at least $t/(2\epsilon)$. The total weight between them can be upper bounded by the total weight of edges connecting C_{true} and C_{false} to the vertices representing gates, which is at most $4 \cdot t \cdot w(0) \leq 16t^2$. Hence, the linkage similarity is at most $16t^2/(t^2/\epsilon^2) = 16\epsilon^2 < \epsilon$.

Next, we show that the gadgets correctly simulate the gates' logic. Suppose $g_k = \mathsf{AND}(g_i, g_j)$ and $\bar{g}_k = \mathsf{OR}(\bar{g}_i, \bar{g}_j)$. Since the edges incident to g_k have higher weights than edges incident to $\bar{g}_k$, g_k are merged first. Below, we consider the *unnormalized* weights, i.e., the weights before normalizing by the product of the cluster weights (comparing unnormalized weights is sufficient since clusters of C_{true} and C_{false} have the same size). Suppose $g_i = g_j = \mathsf{false}$, then the weight between g_k and C_{true} is $w(k)$, the weight to C_{false} is $w(k) + (3/2)\epsilon + 2\epsilon$ and g_k is merged to C_{false}. If only one of $g_i = \mathsf{false}$, then the weight between g_k and C_{true} is $w(k) + \epsilon$, the weight to C_{false} is $w(k) + (3/2)\epsilon + \epsilon$ and g_k will also be merged to C_{false}. Finally, if $g_i = g_j = \mathsf{true}$, the weight between g_k and C_{true} is $w(k) + 2\epsilon$, the weight to C_{false} is $w(k) + (3/2)\epsilon$ and g_k is merged to C_{true}.

Note that when performing the merge for $\bar{g}_k$, the cluster that $\bar{g}_k$ must not merge to has size one larger than the cluster it should merge to. It is easy to calculate as in the example above that this imbalance in sizes does not affect the correctness of the gadget for $\bar{g}_k$.

□

C ParHAC Implementation

This section completes our implementation description introduced in Section C. We implemented ParHAC in C++ using the recently developed *CPAM* (Compressed Parallel Augmented Maps) framework [38], which lets users construct compressed and highly space-efficient ordered maps and sets. We build on CPAM's implementation of the Aspen framework [33, 38], which provides a lossless compressed dynamic graph representation that supports efficient updates (batch edge insertions and deletions). We also use the ParlayLib library for parallel primitives such as reduction, prefix-sum, and sorting [13].

Geometric Layering. Instead of explicitly extracting the edges in each layer and constructing the graph G_c in each outer round, we opted for a simpler approach which works as follows: for each layer-contraction phase in the algorithm we first (i) compute the set of vertices that are active in this phase, i.e., have at least one incident edge in the current layer and then (ii) repeatedly run the capacitated random-mate steps for an inner round from Algorithm 1, recomputing the weights of *all affected edges* in the graph at the end of each inner round. Our implementation modifies Algorithm 1 by removing Line 6, which effectively fuses the outer and inner rounds. After each round, we check whether each vertex is still active, and continue within this layer until no further active vertices remain.

Compressed Clustered Graph Representation. We observed that in practice our ParHAC algorithm can perform a large number of rounds per-layer in the case where ϵ is very small (e.g., $\epsilon = 0.01$). Although updating the entire graph on each of these rounds is theoretically-efficient (the algorithm will only perform $\tilde{O}(m+n)$ work), many of these rounds only merge a small number of vertices, and leave the majority of the edges unaffected. Hence, updating the weights of all edges in each round can be highly wasteful.

Instead, we designed an efficient *compressed clustered graph representation* using purely-functional compressed trees from the CPAM framework [38]. The new data structure handles all merge operations that affect the underlying similarity graph in work proportional to the number of merged vertices and their incident neighbors rather than proportional to the total number of edges in the graph.

Importantly, using CPAM enables lossless compression for integer-keyed maps to store the cluster adjacency information using just a few bytes per edge.[9]

Our data structure stores the vertices in an array, and stores the current neighbors of each vertex in a weight-balanced compressed purely-functional tree called a PaC-tree [38]. Each vertex also stores several extra variables that store its current cluster size, and variables that help build the dendrogram, such as the current cluster-id of each vertex. There are two key operations that we provide in the compressed clustered graph representation:

(1) *MultiMerge*: given a sequence M of (r, b) vertex merges where r is a red vertex and b is a blue vertex, update the graph based on all merges in M.
(2) *Neighborhood Primitives*: apply a function f (e.g., map, reduce, filter) in parallel over all current neighbors of a vertex.

For example, our implementation of Algorithm 1 uses a parallel map operation over the neighbors of all blue vertices to generate a sequence of merges, which it then supplies to the MultiMerge primitive. Additionally, in our implementation, all of the details of maintaining the dendrogram, keeping track of the size of each cluster, and maintaining the current state of the underlying weighted similarity graph are handled by the compressed clustered graph representation. This enables us to write high-level code for our ParHAC implementation while handling the more low-level details about efficiently merging vertices within the clustered graph code.

Other Parallel Graph Clustering Algorithms. Our new graph representation makes it very easy to implement other parallel graph clustering algorithms. In particular, we developed a faithful version of the Affinity clustering algorithm [8] and the recently proposed SCC algorithm [54] (which is essentially a thresholded version of Affinity) using a few dozens of lines of additional code. Both algorithms are essentially heuristics that are designed to mimic the behavior of HAC, while running in very few rounds (an important constraint for the distributed environments these algorithms are designed for). We note that most of the work done by these algorithms is the work required to merge clusters in the underlying graph, and so by using the same primitives for merging graphs, we eliminate a significant source of differences when comparing algorithms.

The Affinity clustering algorithm [8] is inspired by Borůvka's MST algorithm [18]. In each round of Affinity clustering, each vertex selects its heaviest incident edge, and all connected components induced by the chosen edges are merged to form new clusters. This process continues until no further edges remain in the graph. After computing best edges, our implementation uses a highly optimized parallel union-find connectivity algorithm from the ConnectIt framework [34, 43] to compute a unique vertex per Affinity tree, which is used as a 'red' vertex in the MultiMerge procedure, with all other vertices in its component being 'blue' vertices.

The SCC algorithm [54] is closely related to the Affinity algorithm, and can be viewed as running Affinity with different weight thresholds. Specifically, in the i-th round, the SCC algorithm runs a round of Affinity on the graph induced by all edges with weight at least T_i where T_i is the weight threshold on the i-th round. Given the maximum number of rounds R, and the upper threshold U and lower threshold L, the SCC algorithm runs a sequence of R rounds where $T_i = U \cdot (L/U)^{R-i}$. As with Affinity, if the graph becomes empty before all R iterations are run, the algorithm terminates early. We note that our implementation is a best-effort approximation of the SCC algorithm, since SCC was originally designed for the dissimilarity setting and there is no one-to-one mapping to the similarity setting. We refer to our implementation of SCC as SCC_{sim}.

We note that our initial implementations of Affinity and SCC_{sim} were developed in the GBBS framework for static graph processing [32, 36], and did not make use of the compressed clustered graph representation. These initial implementations recomputed the weights of *all* edges in the graph in each round. We found that our new implementations using the compressed clustered graph, which only recompute the weights of edges incident to a merge, are between 7–11x faster across the graphs we evaluate.

[9] We find a 2.9x improvement in space-usage by using our CPAM-based implementation over an optimized hashtable-based implementation of a clustered graph, while the running times of both implementations are essentially the same.

D Experimental Results

Graph Data. We list information about graphs used in our experiments in Table 1. ***com-DBLP (DB)*** is a co-authorship network sourced from the DBLP computer science bibliography (License: *CC BY-SA*). ***YouTube (YT)*** is a social-network formed by user-defined groups on the YouTube site (License: *CC BY-SA*). ***LiveJournal (LJ)*** is a directed graph of the social network (License: *CC BY-SA*). ***com-Orkut (OK)*** is an undirected graph of the Orkut social network (License: *CC BY-SA*). ***Friendster (FS)*** is an undirected graph describing friendships from a gaming network (License: *CC0 1.0*). All of the aforementioned graphs are sourced from the SNAP dataset [51].[10] The licenses are obtained using the data licensing information at the Network Repository.[11] ***USA-Road (RD)*** is an undirected road network from the DIMACS challenge [29] (License: *CC BY-SA*).[12] ***Twitter (TW)*** is a directed graph of the Twitter network, where edges represent the follower relationship [49] (License: *CC BY-SA*). [13] ***ClueWeb (CW)*** is a web graph from the Lemur project at CMU [17] (the authors use a custom open-source license that "provide flexibility to scientists and software developers"; for more details please see `http://www.lemurproject.org/`). [14] ***Hyperlink (HL)*** is a hyperlink graph obtained from the WebDataCommons dataset where nodes represent web pages [53] (License: available to anyone following the Common Crawl Terms of Use: `https://commoncrawl.org/terms-of-use/`). [15] We note that the large real-world graphs that we study are not weighted, and so we set the similarity of an edge (u, v) to $\frac{1}{\log(deg(u)+deg(v))}$. For the CW and HL graphs, which contain tens to hundreds of billions of edges, due to memory constraints on the machine we use, we set the *initial edge weights* to 1 and use byte-codes to store the weights in a number of bytes proportional to their size [69, 38]. We emphasize that the *aggregate weights on edges* (the number of edges in the original graph that each edge between clusters represents) as the algorithm progresses grow *significantly larger*, and do not simply stay fixed at 1.

We also consider graphs generated from a pointset by computing the approximate nearest neighbors (ANN) of each point, and converting the distances to similarities. Our graph building process converts distances to similarities using the formula $\mathsf{sim}(u, v) = \frac{1}{1+\mathsf{dist}(u,v)}$.[16] It then reweights similarities by dividing each similarity by the maximum similarity. In our implementation, we compute the k-approximate nearest neighbors using a shared-memory parallel implementation of the *Vamana* approximate nearest neighbors (ANN) algorithm [44] with parameters $R = 75, L = 100, Q = \max(L, k)$. We note that this parameter setting yields almost perfect recall on the SIFT datasets for the 10-nearest neighbors. More details about the quality of the Vamana algorithm can be found on ANN-Benchmarks [6]. The datasets that we use are sourced from the sklearn.datasets package[17] These datasets are originally sourced from the UCI repository [18], which does not have a clearly stated licensing policy. However, we note that all of the datasets we test on have been widely-used in the machine learning literature, with datsets such as Iris being used in thousands of publications to date. and the Glove-100 dataset from the ANN-Benchmarks collection [6]. The Glove-100 dataset is licensed as Public Domain Dedication and License v1.0.[19] We symmetrized all directed graph inputs studied in this paper.

Experimental Setup. We ran all of our experiments on a 72-core Dell PowerEdge R930 (with two-way hyper-threading) with 4×2.4GHz Intel 18-core E7-8867 v4 Xeon processors (with a 4800MHz bus and 45MB L3 cache) and 1TB of main memory. Our programs use a lightweight parallel scheduler based on the Arora-Blumofe-Plaxton deque [5, 13]. For parallel experiments, we use `numactl -i all` to balance the memory allocations across the sockets.

[10] Sources: `https://snap.stanford.edu/data/`.

[11] https://networkrepository.com/policy.php

[12] http://www.dis.uniroma1.it/challenge9/

[13] Source: `http://law.di.unimi.it/webdata/twitter-2010/`.

[14] Source: `https://law.di.unimi.it/webdata/clueweb12/`.

[15] Source: `http://webdatacommons.org/hyperlinkgraph/`.

[16] We also considered other distance-to-similarity schemes, e.g., $\mathsf{sim}(u, v) = 1/(1 + \log^c(\mathsf{dist}(u, v)))$ and $\mathsf{sim}(u, v) = e^{-\mathsf{dist}(u,v)}$. We observed that the first choice, with $c > 1$ yielded slightly better quality results for sparse graph-based methods, but chose the scheme used in this paper for its simplicity.

[17] For more detailed information see `https://scikit-learn.org/stable/datasets.html`.

[18] `https://archive.ics.uci.edu/ml/datasets.php`

[19] `https://nlp.stanford.edu/projects/glove/`

Table 1: Graph inputs, including the number of vertices (n), number of directed edges (m), and the average degree (m/n).

Graph Dataset	Num. Vertices	Num. Edges	Avg. Degree
com-DBLP **(DB)**	425,957	2,099,732	4.92
YouTube-Sym **(YT)**	1,138,499	5,980,886	5.25
USA-Road **(RD)**	23,947,348	57,708,624	2.40
LiveJournal **(LJ)**	4,847,571	85,702,474	17.6
com-Orkut **(OK)**	3,072,627	234,370,166	76.2
Twitter **(TW)**	41,652,231	2,405,026,092	57.7
Friendster **(FS)**	65,608,366	3,612,134,270	55.0
ClueWeb **(CW)**	978,408,098	74,744,358,622	76.3
Hyperlink **(HL)**	1,724,573,718	124,141,874,032	71.9

D.1 Quality Evaluation

Quality Metrics. To measure quality, we use the ***Adjusted Rand-Index (ARI)*** and ***Normalized Mutual Information (NMI)*** scores, which are standard measures of the quality of a clustering with respect to a ground-truth clustering. We also use the ***Dendrogram Purity*** measure [42], which takes on values between $[0, 1]$ and takes on a value of 1 if and only if the tree contains the ground truth clustering as a tree consistent partition (i.e., each class appears as exactly the leaves of some subtree of the tree). Given a tree T tree with leaves V, and a ground truth partition of V into $C = \{C_1, \ldots, C_l\}$ classes, define the purity of a subset $S \subseteq V$ with respect to a class C_i to be $\mathcal{P}(S, C_i) = |S \cap C_i|/|S|$. Then, the purity of T is

$$\mathcal{P}(T) = \frac{1}{|\textit{Pairs}|} \sum_{i=1}^{l} \sum_{x,y \in C_i, x \neq y} P(\mathsf{lca}_T(x, y), C_i)$$

where $\textit{Pairs} = \{(x, y) \mid \exists i \text{ s.t. } \{x, y\} \subseteq C_i\}$ and $\mathsf{lca}_T(x, y)$ is the set of leaves of the least common ancestor of x and y in T. Lastly, we also study the unsupervised ***Dasgupta Cost*** [27] measure of our dendrograms, which is measured with respect to an underlying similarity graph $G(V, E, w)$ and is defined as:

$$\sum_{(u,v) \in E} |\mathsf{lca}_T(u, v)| \cdot w(u, v)$$

Quality Study. Table 2 shows the results of our quality study. We observe that our $\mathsf{ParHAC}_{0.1}$ algorithm achieves consistent high-quality results across all of the quality measures that we evaluate. For the ARI measure, $\mathsf{ParHAC}_{0.1}$ is on average within 1.5% of the best ARI score for each graph (and achieves the best score for one of the graphs). For the NMI measure, $\mathsf{ParHAC}_{0.1}$ is on average within 1.3% of the best NMI score for each graph (and again achieves the best score for two of the graphs). $\mathsf{ParHAC}_{0.1}$ also achieves good results for the dendrogram purity and Dasgupta cost measures. For purity, it is on average within 1.9% of the best purity score for each graph, achieving the best score for one of the graphs, and for the unsupervised Dasgupta cost measure it is on average within 1.03% of the smallest Dasgupta cost score for each graph. Compared with the SciPy unweighted average-linkage which runs on the underlying pointset, $\mathsf{ParHAC}_{0.1}$ achieves 14.4% better ARI score on average, 3.6% better NMI score on average, 4.7% better dendrogram purity on average, and 1.02% larger Dasgupta cost on average. Lastly, we observe that out of Affinity and SCC_{sim}, SCC_{sim} nearly always outperforms Affinity on all quality measures. Compared to SCC_{sim}, $\mathsf{ParHAC}_{0.1}$ consistently obtains better quality results, achieving 35.6% better ARI score on average, 12.1% better NMI score on average, 6.7% better dendrogram purity on average, and 3.1% better Dasgupta cost on average.

Quality vs. k. We also show additional results for the quality of different algorithms studied in this paper versus the value of k used in the k-NN graph construction. For clarity, the following figures are shown at the end of the appendix.

- Figures 15–18 show quality measures for the *iris* dataset.
- Figures 19–22 show quality measures for the *wine* dataset.
- Figures 23–26 show quality measures for the *digits* dataset.

Table 2: Adjusted Rand-Index (ARI), Normalized Mutual Information (NMI), Dendrogram Purity, and Dasgupta cost of our new ParHAC implementations (columns 2–3) versus the RAC and SeqHAC implementations (columns 4–5), our Affinity and SCC_{sim} implementations (columns 6–7), and the HAC implementations from SciPy (columns 8–11). Both RAC and $\text{SeqHAC}_{\mathcal{E}}$ are exact HAC algorithms, and thus compute the same dendrogram. The scores are calculated by evaluating the clustering generated by each cut of the dendrogram against ground-truth labels. All graph-based implementations are run over the similarity graph given by an approximate k-NN graph with $k = 10$. The Dasgupta cost is computed over the complete similarity graph generated from the all-pairs distance graph. The best quality score for each graph is in green and underlined.

	Dataset	$\text{ParHAC}_{\mathcal{E}}$	$\text{ParHAC}_{0.1}$	RAC and $\text{SeqHAC}_{\mathcal{E}}$	$\text{SeqHAC}_{0.1}$	Affinity	SCC_{sim}	Sci-Single	Sci-Complete	Sci-Avg	Sci-Ward
ARI	*iris*	0.892	0.911	0.873	0.873	0.599	0.786	0.715	0.642	0.759	0.731
	wine	0.401	0.401	0.401	0.401	0.416	0.374	0.298	0.371	0.352	0.368
	digits	0.912	0.896	0.895	0.895	0.625	0.851	0.661	0.479	0.690	0.813
	cancer	0.440	0.491	0.447	0.447	0.375	0.197	0.561	0.465	0.537	0.406
	faces	0.621	0.618	0.610	0.610	0.460	0.607	0.468	0.472	0.529	0.608
NMI	*iris*	0.858	0.876	0.842	0.842	0.692	0.780	0.734	0.722	0.806	0.770
	wine	0.409	0.409	0.394	0.394	0.426	0.400	0.410	0.442	0.428	0.428
	digits	0.928	0.916	0.913	0.931	0.768	0.859	0.562	0.711	0.830	0.869
	cancer	0.445	0.464	0.445	0.445	0.412	0.325	0.316	0.428	0.456	0.423
	faces	0.879	0.874	0.873	0.873	0.858	0.867	0.848	0.849	0.861	0.869
Purity	*iris*	0.931	0.943	0.920	0.920	0.764	0.884	0.843	0.791	0.869	0.850
	wine	0.619	0.623	0.605	0.605	0.616	0.630	0.584	0.607	0.620	0.616
	digits	0.904	0.883	0.891	0.891	0.729	0.811	0.737	0.562	0.755	0.851
	cancer	0.812	0.823	0.797	0.797	0.764	0.703	0.798	0.804	0.829	0.783
	faces	0.640	0.613	0.618	0.621	0.538	0.601	0.566	0.502	0.623	0.614
Dasgupta	*iris*	320665	320883	320665	320665	362177	322308	314445	323384	310957	311267
	wine	29114	29093	29114	29114	29468	27095	27891	27745	27324	26983
	digits	243841216	243166244	243840641	243837090	244130381	244983907	244836138	243726701	240476750	241239871
	cancer	789808	751107	789808	789808	794858	952966	841428	742226	737071	752549
	faces	4629934	4632156	4629934	4622371	4674997	4669787	4640884	4600388	4569916	4619691

Table 3: Variability in each cost measure when running ParHAC using varying values of ϵ on the Iris dataset with $k = 10$. Each entry is the standard deviation of the metric when running 100 repeated trials.

Epsilon	ARI	NMI	Purity	Dasgupta
0	2e−16	3e−16	2e−16	5e−11
0.01	1e−16	3e−16	2e−16	4e−16
0.1	0.058	0.044	0.024	633
1.0	0.063	0.048	0.031	1592

- Figures 27–30 show quality measures for the *faces* dataset.
- Figures 31–34 show quality measures for the *cancer* dataset.

There are several interesting trends that we observe across all of these results:

- First, *sparse similarity graphs*, i.e. graphs constructed using very small k relative to the total number of data points yield high quality results. In particular, using $k = 10$ is almost always an ideal choice for all quality measures except for Dasgupta cost. For the unsupervised Dasgupta cost objective, we observe that the cost actually improves slightly using very dense (almost complete) graphs, which could be due to the fact that the Dasgupta cost measures is computed over the *complete* version of the graph.
- Second, we observe that Affinity and SCC yield significantly more noisy results compared with the ParHAC results (note that Affinity and SCC are deterministic algorithms; by noise we are referring to the clustering quality as a function of k). It would be interesting to better understand why this is the case. We conjecture that this is due to overmerging within each round, and plan to investigate this further in future work.
- Third, ParHAC using $\epsilon = \{0, 0.01, 0.1\}$ yield similar results in terms of quality up until very large k. For $\epsilon = 1$, we see a sharp divergence and loss of quality, which suggests that this value of ϵ may be impractical to use in practice. We find that our suggested choice of $\epsilon = 0.1$ yields almost exact quality results for very sparse graphs (see Table 2 for the results with $k = 10$) and degrades gradually, with poor performance only once the graph becomes close to complete.

Variability for $k = 10$. As ParHAC is a randomized algorithm, the clustering results obtained by the algorithm can vary from run to run. We studied the variability in the clustering outputs obtained by ParHAC for different values of ϵ, and for a fixed $k = 10$ in the graph-building process and show the standard deviation in Table 3. We observe that for $\epsilon = 0$ and very small values, e.g., $\epsilon = 0.01$, the clustering outputs are essentially identical across runs. For $\epsilon = 0.1$, we observe some variability across all cost measures, but note that the difference is at most 5.8% for the ARI, NMI, and Purity metrics, and is just 0.19% of the overall Dasgupta cost for the Dasgupta objective. We also emphasize that the higher variability seems to be responsible for some of the best results that we observe in Table 2, e.g., ParHAC using $\epsilon = 0.1$ achieves the best ARI score across all algorithms that we evaluated. When going from $\epsilon = 0.1$ to $\epsilon = 1$, as expected, we observe that the variability increases with increasing ϵ, as the algorithm has greater choice in which edges to merge in a given layer.

D.2 Scalability Evaluation

In this sub-section, we present additional experimental results on the scalability of our algorithms, both on real-world graph datasets and real-world pointsets (both described earlier).

Speedup Results. In Figure 6 we show the speedup of our ParHAC implementation on the RD, LJ, and OK graphs. On LJ and OK, our ParHAC implementation achieves 48.0x and 61.3x self-relative speedup respectively. For the RD graph, our ParHAC implementation achieves 25.7x self-relative speedup. The lower self-relative speedups for the RD graph are since ParHAC performs significantly less work on RD than on the LJ graph. In particular, the time spent merging vertices in the MultiMerge implementation is 3.8x lower than the time spent in the LJ graph, although both graphs have nearly the same total number of vertices and edges. The reason is that the average number of neighbors per cluster at the time of its merge is significantly lower on RD than on the other graphs.

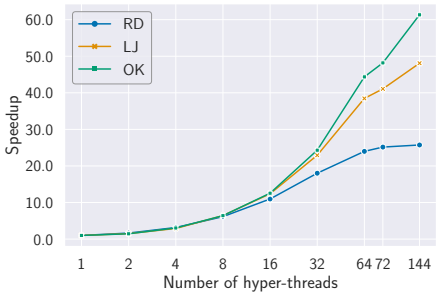


Figure 6: Speedups for three of our large real-world graphs on the y-axis versus the number of hyper-threads used on the x-axis.

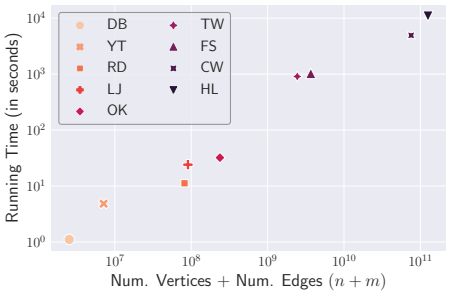


Figure 7: Parallel running time of the ParHAC algorithm in seconds on the y-axis in log-scale versus the size of each graph in terms of the total number of vertices and edges on the x-axis.

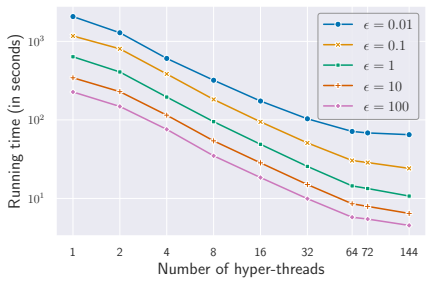


Figure 8: Parallel running times of the ParHAC algorithm on the LJ graph in log-scale as a function of the number of threads for varying values of the accuracy parameter, ϵ.

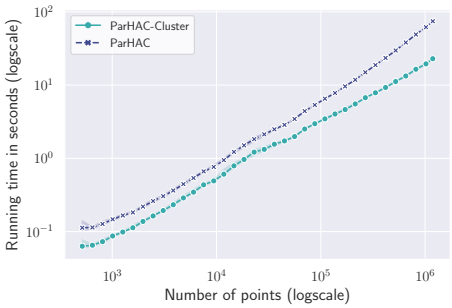


Figure 9: Variability in the end-to-end running times of ParHAC using $\epsilon = 0.1$ and 144 hyper-threads on varying-size slices of the glove-100 dataset. The error lines show the 95% confidence interval for 10 independent runs per point. The running times shown for ParHAC include the cost of computing approximate k-NN and generating the input similarity graph. ParHAC-Cluster reports just the time taken to cluster the generated similarity graph.

Scalability with Increasing Graph Sizes. Figure 7 shows the parallel running times of ParHAC as a function of the graph size in terms of the total number of vertices and edges in the graph. We observe that the running time of our algorithms grows essentially linearly as a function of the graph size. We noticed that although the total number of vertices and edges for the RD and LJ graphs are similar (LJ has 10% more total vertices and edges), the running time for the LJ graph is 33% larger. The reason is that the RD graph has significantly lower average-degree than the LJ graph, which results in much less work being performed on average when merging vertices.

Scalability for Varying Epsilon. In the next experiment, we study the absolute performance and speedup achieved by our ParHAC implementation on a fixed graph, as ϵ is varied. Figure 8 shows the results on the LJ graph for $\epsilon \in \{0.01, 0.1, 1, 10, 100\}$. We observe that larger ϵ consistently results in lower running times, and that the value of $\epsilon = 0.1$ which we use in our quality and other scalability experiments requires the second highest running times. We observed similar results on our other graph inputs. On 144 hyper-threads using a value of $\epsilon = 1$ provides a 2.25x speedup, and $\epsilon = 100$ yields a 5.32x speedup over the parallel running time of $\epsilon = 0.1$.

Performance Variability in End-to-End Experiments. Figure 9 shows the performance variability of our end-to-end experiment from Section 3 (Figure 2). We observe that the performance variability across multiple runs is extremely small, with the exception of the first few data points, which

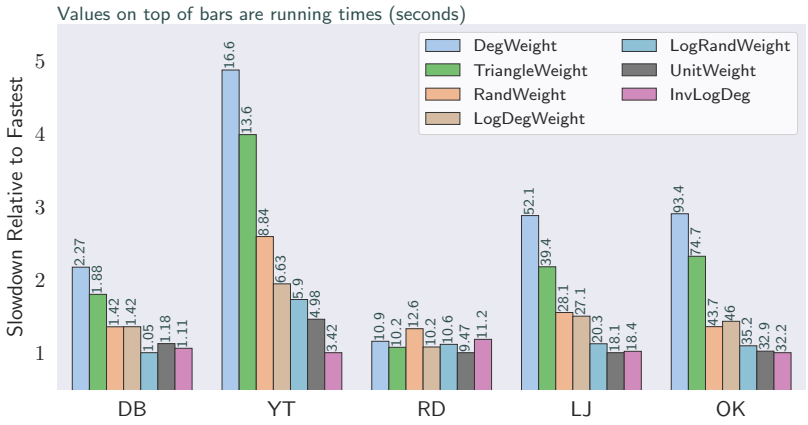


Figure 10: Effect of different weight schemes on the parallel 144-thread running time of ParHAC using $\epsilon = 0.1$.

experience slightly more variability due to scheduling variability when running on very small datasets. Over all slices of the dataset that we evaluate, the largest ratios between the slowest and fastest times for a point is at most $1.31\times$ for the time to run ParHAC, and $1.17\times$ for the end-to-end time, and considering only inputs with $n > 30000$ points, the largest ratios are $9.34\times$ and $4.1\times$ respectively.

Different Weight Schemes. To understand the effect of weights on the performance of ParHAC, we generated five different versions of the RD, LJ, and OK graphs using different weighting schemes where we set the weight of a (u, v) edge as follows:

(1) *DegWeight*: $w(u, v) = deg(u) + deg(v)$
(2) *TriangleWeight*: $w(u, v) = |N(u) \cup N(v)|$
(3) *RandWeight*: $w(u, v) = \mathsf{Uniform}[1, 2^{32}]$
(4) *LogDegWeight*: $w(u, v) = \log(deg(u) + deg(v))$
(5) *LogRandWeight*: $w(u, v) = \log(\mathsf{Uniform}[1, 2^{32}])$
(6) *UnitWeight*: $w(u, v) = 1$
(7) *InvLogDeg*: $w(u, v) = 1/\log(deg(u) + deg(v))$

Note that LogInvWeight is the default weighting scheme used when weighting our unweighted graph inputs.

Figure 10 shows the results of the experiment We found that different weighting schemes has an impact on the running time, but only up to a small constant factor (this is despite the very large difference in the aspect ratios across the different weighting schemes being in some cases). Different weight schemes, especially those based on Degree such as *DegWeight* and *TriangleWeight* require larger overheads on power-law degree distributed graphs like YT, LJ, and OK. In contrast, on RD, all the schemes perform essentially the same, which is due to the fact that the maximum and average-degrees on this graph are a small constant, and since there are very few triangles incident to each edge. Furthermore, we observe that across all graphs, even costly schemes such as *DegWeight* which encourage high-degree vertices to merge with each other can be accurately solved with at most a 5x overhead over schemes like *Unit* or *InvLogDeg*.

Comparison with Other Algorithms. Figure 3 shows the relative performance and parallel running times of ParHAC compared with the SeqHAC and SeqHAC$_{\mathcal{E}}$ algorithms, and our implementations of the RAC, Affinity, and SCC$_{\text{sim}}$ algorithms. We prefix the names of new implementations (where no shared-memory parallel implementation was previously available) with Par.

We observe that our Affinity implementation is always the fastest on our graph inputs. The reason is that on average Affinity requires just 8.7 iterations to complete on these inputs. On the other hand, SCC$_{\text{sim}}$, which runs Affinity with weight thresholding, uses all 100 iterations, and is an average of 11.5x slower than Affinity due to the cost of the additional iterations. Our results show that when carefully implemented, Affinity is a highly scalable algorithms that can cluster graphs with billions of edges in a matter of just tens of minutes, although unlike ParHAC and the other approximate and exact HAC algorithms, they do not provide strong theoretical guarantees.

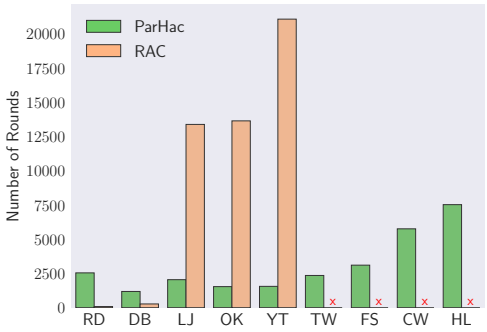


Figure 11: Rounds required by the ParHAC (using $\epsilon = 0.1$) and reciprocal agglomerative clustering (RAC) algorithms for six large real-world graphs. The ClueWeb (CW) and Hyperlink (HL) graphs are two of the largest publicly available graphs, with 978M and 1.72B vertices, and 74B and 124B edges, respectively. We mark experiments where RAC does not finish after 6 hours with a red x.

Compared to Affinity and SCC_{sim}, ParHAC is an average of 14.8x slower than our Affinity implementation and 1.24x slower than our SCC_{sim} implementation. The main reason for the relative speed of ParHAC compared with Affinity is the much larger number of rounds required by ParHAC on our graph inputs (see Figure 11). We note that running SCC_{sim} with fewer rounds yields faster results, but used 100 iterations since this setting yielded the highest quality results in our evaluation in Section 3.1. Furthermore, for all of our graph inputs, Affinity has one (or a few) rounds where the graph shrinks by a massive amount, suggesting the formation of giant cluster(s) through chaining, a known issue with clustering methods based on Boruvka's algorithm [52]. For example, the first round of Affinity on the CW graph drops the number of edges from 74.7B to 5.31B (14x lower) and the number of vertices from 955M to 118M. Importantly, the very first round forms a cluster containing 261M vertices. To conclude, our results show that ParHAC achieves a good compromise between running time and quality, as our study in Section 3.1 shows that both Affinity and SCC_{sim} can produce sub-optimal dendrograms compared to the greedy exact HAC baseline.

Compared with other methods that provide provable guarantees compared with HAC, ParHAC is significantly faster. Compared with SeqHAC and $\text{SeqHAC}_{\mathcal{E}}$, ParHAC obtains 45.2x and 72.7x speedup on average respectively. Compared with RAC, ParHAC achieves an average speedup of 7.1x. Although RAC is faster than ParHAC on DB and RD, two of our small graph inputs, it seems to require a very large number of rounds on the remaining graphs, as we show in Figure 11. In particular, it can take a linear number of steps in the worst case [71], and, as we show in Figure 11, up to 21,081 steps on the YouTube (YT) real-world graph with just 1.1M vertices and 5.9M edges, and an even larger number of rounds on our larger datasets, where RAC does not terminate within 6 hours. Since each round computes the best edge for each vertex for a total of approximately $O(m)$ work, and the number of rounds for our larger graphs is close to $O(\sqrt{m})$ based on Figure 11, the super-linear total work of this algorithm prevents it from achieving good scalability. Similarly, we note that $\text{ParHAC}_{\mathcal{E}}$ (i.e. using $\epsilon = 0$) only runs within the time limit for DB, YT, and RD, and therefore it is not shown in Figure 3. The reason is that it performs $O(mn)$ work when $\epsilon = 0$, since each iteration costs $O(m)$ work and the number of outer-rounds is $O(n)$.

Discussion. To the best of our knowledge, our results are the first to show that graphs with tens to hundreds of billions of edges can be clustered in a matter of tens of minutes (using heuristic methods like Affinity and SCC_{sim} with fewer iterations) to hours (using SCC_{sim} with many iterations or methods with approximation guarantees such as ParHAC). We are not aware of other shared-memory clustering results that work at this large scale. Our theoretically-efficient implementations can be viewed as part of a line of work showing that theoretically-efficient shared-memory parallel graph algorithms can scale to the largest publicly available graphs using a modest amount of resources [31–33].

D.3 Ablation: Comparing CPAM with Hash-based Representations

When designing our implementation of ParHAC, and specifically the clustered graph representation, we also considered other implementations of a clustered graph. Specifically, we considered other ways of representing the out-neighborhood of a vertex (cluster). To better understand the impact of using

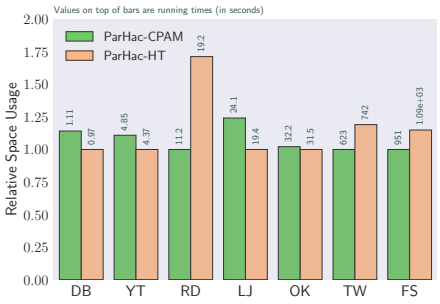


Figure 12: Relative running times of ParHAC-CPAM (cluster neighborhoods represented using compressed purely-functional trees from the CPAM framework) and ParHAC-HT (cluster neighborhoods represented using parallel hashtable). The values shown on top of each bar are the running time in seconds using 144 hyper-threads.

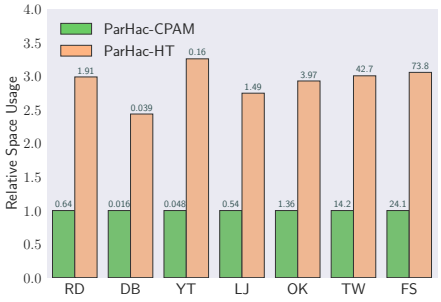


Figure 13: Relative sizes of the memory representation in bytes of ParHAC-CPAM (cluster neighborhoods represented using compressed purely-functional trees from the CPAM framework) and ParHAC-HT (cluster neighborhoods represented using parallel hashtables). Weights are stored as uncompressed floats. The values shown on top of each bar are the space usage of each representation in gigabytes (GiB).

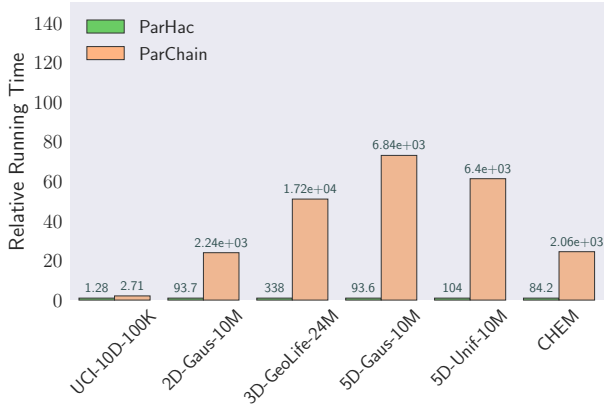


Figure 14: Performance of ParHAC compared with ParChain on the large low-dimensional pointset inputs used in the ParChain paper. The running times for ParHAC include the similarity graph construction time.

CPAM to represent this weighted adjacency information, we implemented a new *hashtable-based* implementation of the clustered graph object where each cluster stores its neighbors in a hashtable (table). Our hashtable representation uses the linear-probing concurrent hashtable described by Shun et al. [67] to represent the weights. In our implementation of a hash-based clustered graph, each hashtable is keyed by the id of the neighbor and the value stored is the weight of the edge. We call the CPAM-based implementation ParHAC-CPAM and the hashtable-based implementation ParHAC-HT.

To understand the impact of using CPAM, we studied the parallel running time of our algorithms using ParHAC-CPAM and ParHAC-HT, as well as the space usage of both types of representations. Figure 12 and Figure 13 show the relative running times and relative sizes, respectively. We find that the two implementations achieve very similar running times across all graphs (the one notable exception is the RD graph, which has very low average degree, and therefore results suffers some overhead due to hashing in the hashtable-based implementation). On the other hand, the space usage of ParHAC-CPAM is consistently much better than that of ParHAC-HT, with an average space improvement of 2.9x.

D.4 Comparing ParHAC with ParChain

In addition to our comparison with Fastcluster in the main text of the paper, we wanted to understand how ParHAC compares with state-of-the-art multicore parallel metric HAC implementations. We

selected ParChain [75], since this recent algorithm demonstrates performance improvements over other existing parallel implementations of metric HAC.

To understand how ParHAC and ParChain compare, we ran ParHAC on a subset of the largest pointset datasets used in the ParChain paper [75], using the same end-to-end approach described earlier (graph building using an implementation of Vamana, followed by running ParHAC). Figure 14 shows the results of the experiment. We find that on average, ParHAC is 39.3x faster, and up to 73x faster than ParChain for the average-linkage measure. We note that when we tried to run ParChain on the same high-dimensional inputs used in this paper, e.g., Glove-100, the algorithm crashed, which is likely due to the fact that ParChain and its optimizations were designed for low-dimensional (approximately $d \leq 16$) HAC. We also ran ParChain on the UCI datasets, and found that it produced identical dendrograms to those computed by Sklearn, FastCluster, and SciPy, confirming that ParChain is an exact algorithm (and is implemented correctly).

The datasets used in our experiments can be found in the ParChain paper, and are also described below for completeness:

ParChain Datasets. The ***GaussianDisc*** data set contains points inside a bounding hypergrid with side length $5\sqrt{n}$, where n is the total number of points. 90% of the points are equally divided among five clusters, each with a Gaussian distribution. Each cluster has its mean randomly sampled from the hypergrid, a standard deviation of $1/6$, and a diameter of $\sqrt{n}$. The remaining points are randomly distributed. The ***UniformFill*** data set contains points distributed uniformly at random inside a bounding hypergrid with side length $\sqrt{n}$, where n is the total number of points. These datasets are synthetically generated, and thus no license is applicable to the best of our knowledge. The synthetic data sets contain 10 million points for dimensions $d = 2$ and $d = 5$. Lastly, ***UCI1*** [3, 16] is a 10-dimensional data set with 19020 data points.

GeoLife [76, 2] is a 3-dimensional real-world data set with 24876978 points. This dataset contains user location data, and is extremely skewed. The data is provided as part of a Microsoft Research project, and no license information is available online to the best of our knowledge. ***CHEM*** [39, 1] is a 16-dimensional dataset with 4208261 points containing chemical sensor data. Similar to the other datasets from UCI, no licensing information is available, although the project states that the dataset has been donated to UCI by the creators of the dataset (from UCSD).

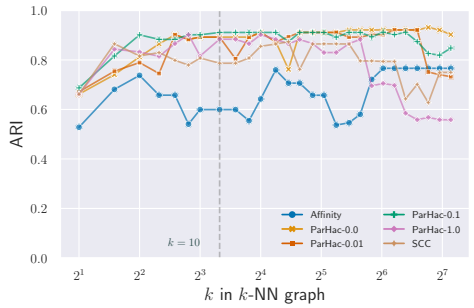


Figure 15: Adjusted Rand-Index (ARI) of clusterings computed by ParHAC for varying ϵ on Iris versus the k used in similarity graph construction.

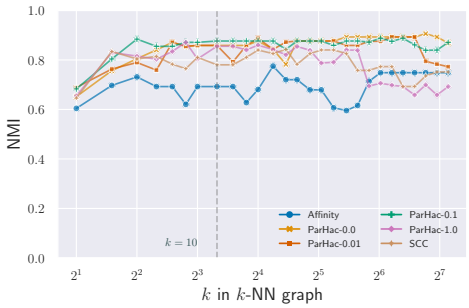


Figure 16: Normalized Mutual Information (NMI) of clusterings computed by ParHAC for varying ϵ on Iris versus the k used in similarity graph construction.

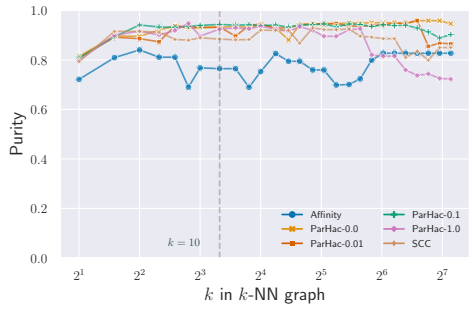


Figure 17: Dendrogram Purity (Purity) of clusterings computed by ParHAC for varying ϵ on Iris versus the k used in similarity graph construction.

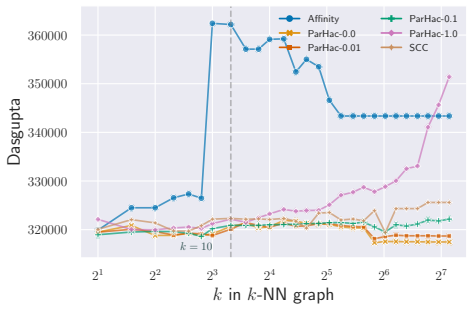


Figure 18: Dasgupta Cost (Dasgupta) of clusterings computed by ParHAC for varying ϵ on Iris versus the k used in similarity graph construction.

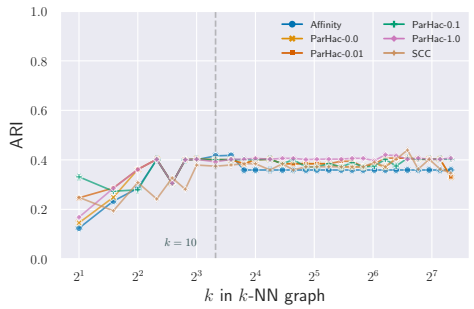


Figure 19: Adjusted Rand-Index (ARI) of clusterings computed by ParHAC for varying ϵ on Wine versus the k used in similarity graph construction.

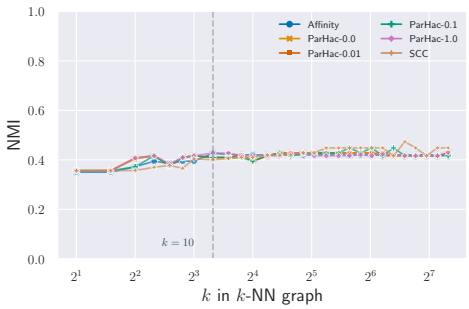


Figure 20: Normalized Mutual Information (NMI) of clusterings computed by ParHAC for varying ϵ on Wine versus the k used in similarity graph construction.

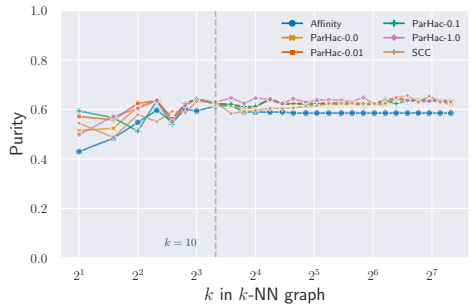


Figure 21: Dendrogram Purity (Purity) of clusterings computed by ParHAC for varying ϵ on Wine versus the k used in similarity graph construction.

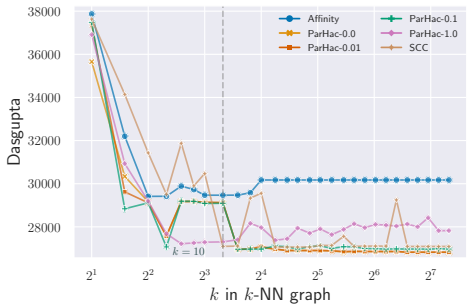


Figure 22: Dasgupta Cost (Dasgupta) of clusterings computed by ParHAC for varying ϵ on Wine versus the k used in similarity graph construction.

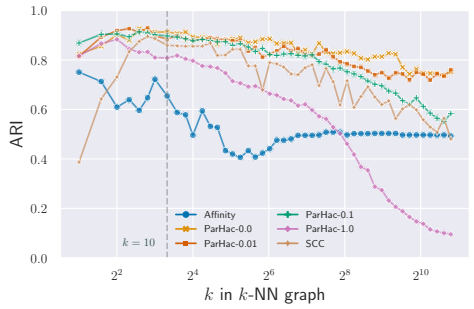


Figure 23: Adjusted Rand-Index (ARI) of clusterings computed by ParHAC for varying ϵ on Digits versus the k used in similarity graph construction.

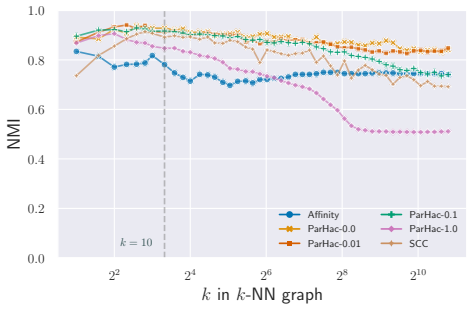


Figure 24: Normalized Mutual Information (NMI) of clusterings computed by ParHAC for varying ϵ on Digits versus the k used in similarity graph construction.

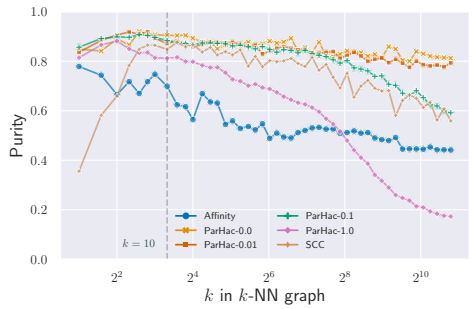


Figure 25: Dendrogram Purity (Purity) of clusterings computed by ParHAC for varying ϵ on Digits versus the k used in similarity graph construction.

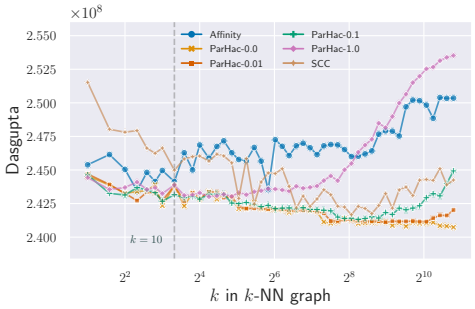


Figure 26: Dasgupta Cost (Dasgupta) of clusterings computed by ParHAC for varying ϵ on Digits versus the k used in similarity graph construction.

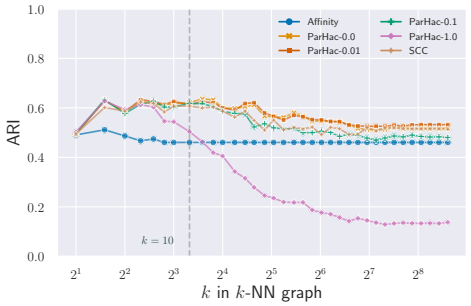


Figure 27: Adjusted Rand-Index (ARI) of clusterings computed by ParHAC for varying ϵ on Faces versus the k used in similarity graph construction.

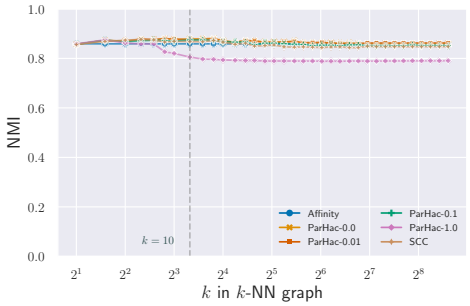


Figure 28: Normalized Mutual Information (NMI) of clusterings computed by ParHAC for varying ϵ on Faces versus the k used in similarity graph construction.

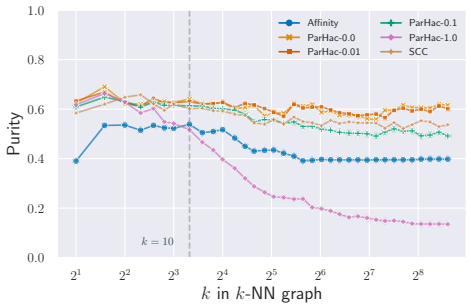


Figure 29: Dendrogram Purity (Purity) of clusterings computed by ParHAC for varying ϵ on Faces versus the k used in similarity graph construction.

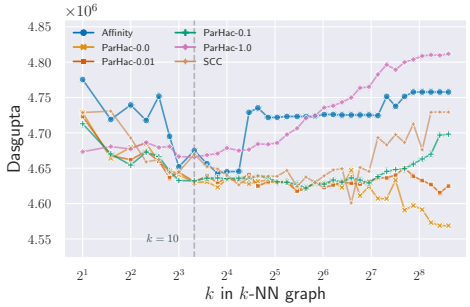


Figure 30: Dasgupta Cost (Dasgupta) of clusterings computed by ParHAC for varying ϵ on Faces versus the k used in similarity graph construction.

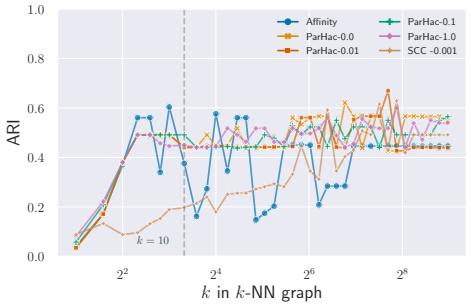


Figure 31: Adjusted Rand-Index (ARI) of clusterings computed by ParHAC for varying ϵ on Cancer versus the k used in similarity graph construction.

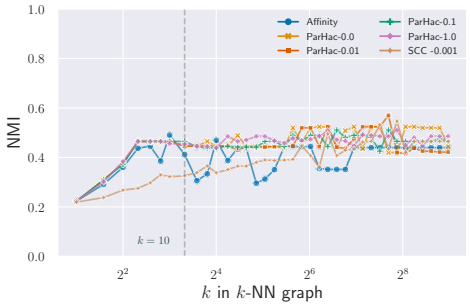


Figure 32: Normalized Mutual Information (NMI) of clusterings computed by ParHAC for varying ϵ on Cancer versus the k used in similarity graph construction.

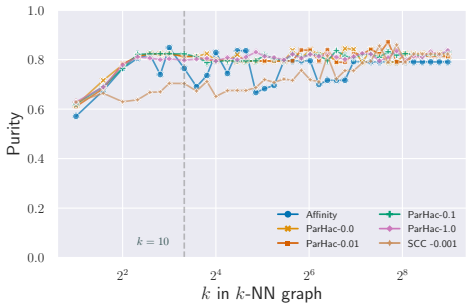


Figure 33: Dendrogram Purity (Purity) of clusterings computed by ParHAC for varying ϵ on Cancer versus the k used in similarity graph construction.

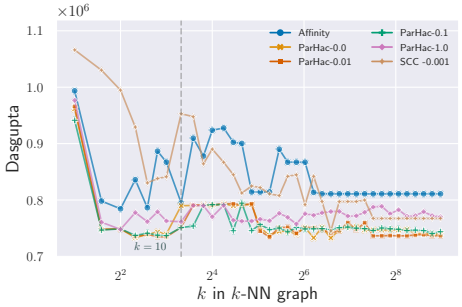


Figure 34: Dasgupta Cost (Dasgupta) of clusterings computed by ParHAC for varying ϵ on Cancer versus the k used in similarity graph construction.